



REPUBLIC OF TÜRKİYE
ALTINBAŞ UNIVERSITY
Institute of Graduate Studies
Mechanical Engineering

**ADVANCED STRUCTURAL ANALYSIS OF UAV
PERFORMANCE USING COMPOSITE
MATERIALS**

Adian Waleed Ismail ISMAIL

Master's Thesis

Supervisor

Asst. Prof. Dr. Yaser ALAIWI

Istanbul, 2024

**ADVANCED STRUCTURAL ANALYSIS OF UAV
PERFORMANCE USING COMPOSITE MATERIALS**

Adian Waleed Ismail ISMAIL

Mechanical Engineering

Master's Thesis

ALTINBAŞ UNIVERSITY

2024

The thesis titled ADVANCED STRUCTURAL ANALYSIS OF UAV PERFORMANCE USING COMPOSITE MATERIALS prepared by ADIAN WALEED ISMAIL ISMAIL and submitted on 04/06/2024 has been **accepted unanimously** for the degree of Master of Science in Mechanical Engineering.

Asst. Prof. Dr. Yaser ALAIWI
Supervisor

Thesis Defense Committee Members:

Asst. Prof. Dr. Yaser ALAIWI

Department of Mechanical
Engineering,
Altınbaş University

Asst. Prof. Dr. Abdullahi Abdu
IBRAHIM

Department of Computer
Engineering,
Altınbaş University

Asst. Prof. Dr. Haydar İzzettin
KEPEKÇI

Department of Mechanical
Engineering,
Istanbul Gelisim University

I hereby declare that this thesis meets all format and submission requirements for a Master's thesis.

I hereby declare that all information/data presented in this graduation project has been obtained in full accordance with academic rules and ethical conduct. I also declare all unoriginal materials and conclusions have been cited in the text and all references mentioned in the Reference List have been cited in the text, and vice versa as required by the abovementioned rules and conduct.

Adian Waleed Ismail ISMAIL

Signature



DEDICATION

I want to dedicate this thesis to my respected supervisor Asst. Prof. Dr. Yaser ALAIWI has always supported, advised, and guided my way in research. Your contribution of invaluable ideas and mentorship to this work is immeasurable but has also given me the impetus to break the boundaries of knowledge in the field of mechanical engineering.

Besides, I would like to express my sincere thanks to the distinguished faculty members of the Department of Mechanical Engineering at Altınbaş University. Your passion for the standards of excellence in education and research has laid a good foundation and equipped me with the tools I need to accomplish this.

This Thesis is dedicated to my family and friends as proof of your love, support, and belief in me. Your continuous help is the spirit that makes me persist and have the courage to fight challenges and reach my objectives.

All who have been instrumental in my academic and personal development are to be honoured by the evil book that is my thesis, and I am forever grateful.

ABSTRACT

ADVANCED STRUCTURAL ANALYSIS OF UAV PERFORMANCE USING COMPOSITE MATERIALS

ISMAIL, Adian Waleed Ismail

M.Sc., Mechanical Engineering, Altınbaş University,

Supervisor: Asst. Prof. Dr. Yaser ALAIWI

Date: June/2024

Pages: 83

This research examines the capability of composite materials to improve the structural and aerodynamic characteristics of the wing of AAI Shadow 200 RQ-7 unmanned aerial vehicle (UAV). The study applies an extensive numerical analysis approach, using Computational Fluid Dynamics (CFD), Fluid-Structure Interaction (FSI), and also modal analysis methods to evaluate the wing performance under different loading situations. The UAV wing is designed and modelled with SolidWorks software, while the numerical simulations are carried out using ANSYS. The study measures the performance of the wing made through conventional aluminium construction against the wing made with Epoxy Carbon UD Prepreg and Epoxy/glass fibre UD prepreg QI composite materials. The test results show that the combination of composite material group realized significant enhancement of the structural performance of the wing of UAVs, with QI composite of Epoxy/glass fibre UD prepreg obtaining the remarkable performance of higher safety factors, less deformation, and the better ability of bearing loads. The modal analysis showed the similar effects of both composite materials on the vibration behaviour of the wing. This study reveals the opportunity of the composites in improving UAV wing design and stresses the role of numerical analysis methods in the creation of modern UAVs.

Keywords: CFD, FSI, Composite Materials, UAV, Modal Analysis.

TABLE OF CONTENTS

	<u>Pages</u>
ABSTRACT	vi
LIST OF TABLES	x
LIST OF FIGURES	xi
ABBREVIATIONS	xiv
LIST OF SYMBOLS	xv
1. INTRODUCTION	1
1.1 BACKGROUND	1
1.2 MOTIVATION.....	2
1.3 THESIS OBJECTIVES.....	3
1.4 SCOPE OF THE STUDY	4
1.5 THESIS STRUCTURE.....	4
2. LITERATURE REVIEW	6
3. METHODOLOGY	23
3.1 AERODYNAMICS	23
3.1.1 Introduction	23
3.1.2 Concepts	24
3.2 COMPUTATIONAL FLUID DYNAMICS	26
3.2.1 Introduction	26
3.2.2 Governing Equations.....	27
3.3 FLUID STRUCTURE INTERACTION.....	28
3.3.1 Introduction	28
3.4 FINITE ELEMENT METHOD.....	30

3.4.1 Introduction	30
3.4.2 Finite Element Methods Steps	30
3.4.3 Finite element Application	32
3.4.4 ANSYS Software	32
3.5 COMPOSITE MATERIAL.....	33
3.5.1 Introduction	33
3.5.2 Classifications of Composite Materials	34
3.5.3 Using Composite Materials in Aerospace Applications	35
3.5.4 Failure Criteria.....	36
3.5.4.1 Maximum stress criterion	36
3.5.4.2 Maximum strain criterion	36
3.5.4.3 Tsai-Wu failure criterion	37
3.5.4.4 Tsai-Hill failure criterion.....	38
3.5.4.5 Inverse reverse factor and safety factor.....	38
3.6 NATURAL FREQUENCY	39
3.6.1 Introduction	39
3.6.2 Natural Frequency Formulas	39
3.7 AAI SHADOW -200 RQ-7 UAV DESIGN AND NUMERICAL ANALYSIS.....	40
3.7.1 AAI Shadow -200 RQ-7 UAV Design.....	41
3.7.2 AAI Shadow -200 RQ-7 UAV Numerical Analysis.....	44
3.7.2.1 CFD analysis.....	45
3.7.2.2 FSI analysis.....	47
3.7.2.3 ACP composite materials analysis	48
3.7.2.4 Modal analysis	49
4. RESULTS AND DISCUSSION	50

4.1 CFD ANALYSIS RESULTS	50
4.2 FIRST CASAE STUDY RESULTS	53
4.2.1 FSI Analysis Results	53
4.2.2 Modal Analysis Results	55
4.3 SECOND CASAE STUDY RESULTS	56
4.3.1 FSI Analysis Results	56
4.3.2 Modal Analysis Results	58
4.4 THIRD CASAE STUDY RESULTS	59
4.4.1 FSI Analysis Results	59
4.4.2 Modal Analysis Results	61
5. CONCLUSIONS AND RECOMMENDATIONS	63
5.1 CONCLUSIONS	63
5.2 RECOMMENDATIONS	63
REFERENCES	65

LIST OF TABLES

	<u>Pages</u>
Table 3.1: Dimensions of RQ-7 UAV.	41
Table 3.2: Properties of the Fluid Domain.	44
Table 3.3: Mesh Settings for Fluid Domain.	45
Table 3.4: ANSYS Fluent Analysis Setup Settings.	46
Table 3.5: Composite, Epoxy Carbon UD (230 Gpa) Prepreg .[64]	48
Table 3.6: Composite, Epoxy/Glass Fiber, UD Prepreg, QI [65].	48
Table 4.1: Results of CFD Analysis	52
Table 4.2: Results of FSI Analysis for First Case.	54
Table 4.3: Natural Frequencies of First Case Study.	55
Table 4.4: Results of FSI Analysis for Second Case.	58
Table 4.5: Safety Factors Values for Different Criterias for Second Case.	58
Table 4.6: Inverse Reserve Factor Values for Different Criterias for Second Case.	58
Table 4.7: Natural Frequencies of Second Case Study.	59
Table 4.8: Results of FSI Analysis for Third Case.	61
Table 4.9: Safety Factors Values for Different Criterias for Third Case.	61
Table 4.10: Inverse Reserve Factor Values for Different Criterias for Third Case.	61
Table 4.11: Natural Frequencies of Third Case Study.	62

LIST OF FIGURES

	<u>Pages</u>
Figure 3.1: Boundary Layer on Fixed Wing of Aircraft [44].....	25
Figure 3.2: Different Forces that Affect the Aircraft's Fixed Wing [45].	26
Figure 3.3: Some of CFD Applications in Different Fields [47].....	27
Figure 3.4: FSI Analysis Workflow [50].	29
Figure 3.5: (A) One-Way and (B) Two-Way Interaction Approaches for Fluid-Structure Integration [49].	30
Figure 3.6: Shows the Stress-Strain Relationships Under Uniaxial and Shear Loading Conditions, Highlighting the in-Plane Strengths and Ultimate Strain Limits of A Lamina [55].	37
Figure 3.7: Shows the Failure Surfaces for the Maximum Stress, Maximum Strain, and Tsai-Hill Criteria in Σ_1 , Σ_2 Stress Space, Demonstrating How Each Criterion Predicts the Material Failure Under Different Stress Conditions [55].....	38
Figure 3.8: AAI Shadow -200 RQ-7 UAV [62].	41
Figure 3.9: AAI Shadow -200 RQ-7 UAV Model.....	41
Figure 3.10: Dimensions of Wingspan.	42
Figure 3.11: Dimensions of Total Length.	42
Figure 3.12: AAI Shadow -200 RQ-7 Wing Length.....	43
Figure 3.13: RQ 7 UAV in Fluid Domain.....	43
Figure 3.14: RQ 7 UAV Wing in the Fluid Domain.....	43
Figure 3.15: Mesh Results on Whole Fluid Domain.	45
Figure 3.16: Mesh Results on Whole Fluid Domain.	45
Figure 3.17: Boundary Conditions of Fluid Domain for RQ-7.....	46
Figure 3.18: Mesh Results on 3D Wing of RQ-7 UAV.....	47

Figure 3.19: (A) Shows the Fixed Support and (B) the Imported Pressure Load on the RQ-7 UAV.....	47
Figure 3.20: RQ-7 Wing After Composite Material Added.....	48
Figure 3.21: Project Schematic for the First Case Study.	49
Figure 3.22: Project Schematic for the Second and Third Case Study.....	49
Figure 4.1: Convergence of Solution of CFD Analysis.	50
Figure 4.2: Value of Drag Coefficient Against Solution Iterations.....	51
Figure 4.3: Value of Drag Force Against Solution Iterations.	51
Figure 4.4: Value of Lift Coefficient Against Solution Iterations.....	51
Figure 4.5: Value of Lift Force Against Solution Iterations.	51
Figure 4.6: Shows the Pressure Contours on the 3D Wing.....	52
Figure 4.7: Shows the Pressure Contours on the 2D Section of Wing.	52
Figure 4.8: Maximum Von-Mises Stress on RQ-7 Wing When the Material is Aluminium.	53
Figure 4.9: Total Deformation on RQ-7 Wing When the Material is Aluminium.....	53
Figure 4.10: Equivalent Elastic Strain on RQ-7 Wing When the Material is Aluminium.	53
Figure 4.11: Strain Energy of RQ-7 Wing When the Material is Aluminium.	54
Figure 4.12: Safety Factor of RQ-7 Wing When the Material is Aluminium.....	54
Figure 4.13: Modal Analysis Results Of RQ-7 Wing When the Material is Aluminium: (A) Mode 1, (B) Mode 2 , (C) Mode 3, (D) Mode 4, (E) Mode 5	55
Figure 4.14: Maximum Von-Mises Stress On RQ-7 Wing When the Material is Composite, Epoxy Carbon UD (230 Gpa) Prepreg.....	56
Figure 4.15: Total Deformation On RQ-7 Wing When the Material is Composite, Epoxy Carbon UD (230 Gpa) Prepreg.....	56
Figure 4.16: Equivalent Elastic Strain on RQ-7 Wing When the Material is Composite, Epoxy Carbon UD (230 Gpa) Prepreg.....	56

Figure 4.17: Strain Energy Of RQ-7 Wing When the Material Is Composite, Epoxy Carbon UD (230 Gpa) Prepreg.	57
Figure 4.18: Safety Factor Of RQ-7 Wing When the Material is Composite, Epoxy Carbon UD (230 Gpa) Prepreg.	57
Figure 4.19: Inverse Reserve Factor Of RQ-7 Wing When the Material is Composite, Epoxy Carbon UD (230 Gpa) Prepreg.	57
Figure 4.20: Modal Analysis Results of RQ-7 Wing When the Material is Composite, Epoxy Carbon UD (230 Gpa) Prepreg.: (A) Mode 1, (B) Mode 2 , (C) Mode 3, (D) Mode 4, (E) Mode 5.	58
Figure 4.21: Total Deformation on RQ-7 Wing When the Material is Composite, Epoxy/Glass Fiber, UD Prepreg, QI.	59
Figure 4.22: Equivalent Elastic Strain On RQ-7 Wing When the Material is Composite, Epoxy/Glass Fiber, UD Prepreg, QI.	59
Figure 4.23: Strain Energy Of RQ-7 Wing When the Material is Composite, Epoxy/Glass Fiber, UD Prepreg, QI.	60
Figure 4.24: Safety Factor of RQ-7 Wing When the Material is Composite, Epoxy/Glass Fiber, UD Prepreg, QI.	60
Figure 4.25: Inverse Reserve Factor of RQ-7 Wing When the Material is Composite, Epoxy/Glass Fibre, UD Prepreg, QI.	60
Figure 4.26: Modal Analysis Results of RQ-7 Wing When the Material is Composite, Epoxy/Glass Fiber, UD Prepreg, QI. (A) Mode 1, (B) Mode 2 , (C) Mode 3, (D) Mode 4, (E) Mode 5.	61
Figure 4.27: AAI Shadow -200 RQ-7 UAV Model After Adding Composite Material.	62

ABBREVIATIONS

CAD	:	Computer-Aided Design
CFD	:	Computational Fluid Dynamics
FEM	:	Finite Element Method
UAV	:	Unmanned Aerial Vehicle
IRF	:	Inverse Reverse Factor
CMC	:	Composed of Ceramic fibre
PMC	:	Polymer Matrix Composites
MMC	:	Metal Matrix Composite
FSI	:	Fluid Structure Interaction

LIST OF SYMBOLS

C_D	:	Drag Coefficient
F_d	:	Drag Force
ρ	:	Fluid Density
v	:	Velocity of Fluid
A	:	Base Area
p	:	Pressure.
L	:	Lift Force
C_L	:	Lift Coefficient
α	:	Angle of Attack
V_{stall}	:	Stall Speed
g	:	Gravitational Constant
τ	:	Viscous Stresses
q	:	Heat Flux
σ_1	:	Longitudinal Stress
σ_2	:	Transverse Stress
τ_{12}	:	Shear Stress
ϵ_1	:	Longitudinal Strain
ϵ_2	:	Transverse Strain
n	:	Safety Factor
f	:	Natural Frequency
μ	:	Mass Per Unit Length
E	:	Young's Modulus

1. INTRODUCTION

1.1 BACKGROUND

UAVs or drones are systems that use aircraft to function without a human pilot en route. They're remotely controlled or fly autonomously using software-controlled flight plans in their onboard systems operating in sync with onboard sensors and GPS. UAVs are one of Unmanned Aerial Systems (UAS) that encompasses the UAV, the ground-based controller and the network of communications between them. The technology of UAVs includes different kinds of vehicles, which range from small consumer drones to large military UAVs, and is employed for various uses such as surveillance, delivery, and environmental monitoring [1].

The development of Unmanned Aerial Vehicles (UAVs) is an impressive story from the early 1900s to the contemporary systems used. The idea of UAVs was first born in the need to decrease human losses in battlefields as a result of which such devices as the Kettering Bug were created in World War I, an obscure though revolutionary flying bomb. During the interwar years and World War II, UAV technology advanced remarkably. Advancements during this period consisted of the remotely controlled target aircraft. One example of such an aircraft is the British-developed Queen Bee, which provided a safer way of training anti-aircraft gunners. The Cold War era highlighted the importance of UAVs for clandestine reconnaissance becoming the era of the Lightning Bug that performed surveillance missions outside enemy lines. It was during this period that the focus started changing in favour of the possibilities of using UAVs for intelligence gathering without risking human lives directly. The Vietnam War era also underlined the operational utility of UAVs as drones like the Firebee became used for reconnaissance. The same period marked the use of UAVs in electronic warfare that could jam enemy communications and gather signals intelligence, highlighting their increasing flexibility. Towards the end of the 20th century, technological progress made it possible to produce more advanced and dependable UAVs, which could conduct various missions. This was inclusive of intelligence collection, battlefield reconnaissance, as well as electronic warfare, showing UAVs' broader role beyond traditional military operations. UAVs or drones such as the Predator and Reaper have become essential in the 21st century to military strategies across the globe, and they can conduct surveillance, targeted strikes, and real-time data. The performance of these UAVs

in different conflicts unarguably positions them as important modern warfare tools which provide precision functions with a very low human risk. Today, the utilization of UAVs is not relegated to military purposes, rather it has extended to disaster response, environmental monitoring, and even civil purposes, signifying how they transitioned from experimental toys to flexible flying tools. The development history reflects not only technological improvements but also the dynamic nature of conflict and the unceasing search for better and safer operational methods [2].

Different sectors greatly benefit from Unmanned Aerial Vehicles (UAVs), evidencing their versatility and efficiency. The UAVs revolutionize traditional farming practices in agriculture where they provide soil analysis in detail, assess crop health, deliver targeted spray treatments, and manage irrigation systems efficiently. They provide rapid damage assessment which is very important for the response and recovery process. In operation of the military, UAVs are used for oversight, air strikes, bomb identification, and maintaining security thus reducing human risk and increasing the efficiency of the mission. Civilian uses of UAVs are also broad and may include photography, shipping and delivery, disaster rescue operations, archaeological surveys, geographic mapping, health monitoring, livestock surveillance, safety inspections and atmospheric research. Each of these uses illustrates the UAV's ability to carry out tasks that are unsafe, time-consuming, or extremely difficult to human beings, emphasizing the UAV's role in technology development and its utility in different areas [3].

1.2 MOTIVATION

- a. The fast development and innovation of the unmanned aerial vehicle (UAV) industry have resulted in the increasing demand for better structural performance and aerodynamic efficiency of the UAV components, especially, the wings.
- b. Aluminium and other traditional materials have problems with structural performance, weight, and aerodynamics, and therefore pose challenges to the utilization of UAVs in various applications.
- c. Composite materials, characterized by their high strength, durability, light weight and ability to customise, are a good solution to the drawbacks of traditional materials in UAV wing design.

- d. Although the demand for the use of composite materials for UAV is increasing, there is an absence of detailed research that are focused on the application of composite materials in the UAV wing design.
- e. This research seeks to fill this void by conducting a thorough study on the suitability of various composite materials in improving the structural and aerodynamic performance of the AAI Shadow-200 RQ-7 UAV wing.
- f. The research utilizes modern numerical analysis methods such as Computational Fluid Dynamics (CFD), Fluid-Structure Interaction (FSI), and modal analysis to evaluate the performance of the UAV wing under different loading cases.
- g. The results of this research can revolutionize UAV wing design and development by determining the best composite material configuration for enhanced performance and safety.
- h. The comprehensive method used in this research which involves the use of several numerical analysis techniques and comparison of different composite materials, provides a good base for additional research in the area of composite materials for UAV applications.

1.3 THESIS OBJECTIVES

- a. To construct an accurate CAD model of the shell-and-tube heat exchanger and carry out nanofluid CFD simulations to quantify efficiency improvements.
- b. To create and simulate using SolidWorks software the wing of the AAI Shadow-200 RQ-7 UAV, ensuring that all the dimensions and geometry are correct for further numerical studies.
- c. To analyse the aerodynamic behaviour of the UAV wing under different loading conditions using the ANSYS software for computational fluid dynamics (CFD), with a particular focus on the identification of lift and drag forces on the wing.
- d. To analyse the structural behaviour of the UAV wing under aerodynamic loads using Fluid-Structure Interaction (FSI) analysis, taking into account both aluminium and composite material layouts.
- e. To evaluate the structural performance of the UAV wing made of the traditional aluminium construction with the wing that includes Epoxy Carbon UD Prepreg and Epoxy/glass fibre UD prepreg QI composite materials in stress distribution, deformation, and safety factors.

- f. To determine the vibrational performance of the UAV wing with and without composite materials through modal analysis to obtain the natural frequencies and mode shapes of the wing structure.
- g. Determining the most appropriate composite material configuration based on the numerical analysis results for the AAI Shadow-200 RQ-7 UAV wing, taking into account the structural performance, aerodynamic efficiency, and safety margins.
- h. To provide useful comments and suggestions on the design and production of the advanced UAV wings made of composite materials, as a contribution to the developing collection of UAV technology and composite material application in the industry.

1.4 SCOPE OF THE STUDY

- a. The research is restricted to the numerical study of the AAI Shadow-200 RQ-7 UAV wing utilizing Computational Fluid Dynamics (CFD), Fluid-Structure Interaction (FSI), and modal analysis methodologies.
- b. The composite materials under consideration in this study are Epoxy Carbon UD Prepreg and Epoxy/glass fibre UD prepreg QI.
- c. The structural performance, aerodynamic efficiency and vibrational characteristics of the UAV wing are the main issues under investigation in the study.
- d. The numerical computations are carried out with SolidWorks for design and modelling and ANSYS software for CFD, FSI, and modal analysis.
- e. The UAV wing geometry is modelled based on the existing AAI Shadow-200 RQ-7 design, with modifications made to accommodate the application of composite materials.

1.5 THESIS STRUCTURE

Chapter 1 - Introduction: Provides an overview of the research, including background, motivation, objectives, and scope.

Chapter 2 - Literature Review: Presents a review of existing literature related to UAV technology, wing design, composite materials, and numerical analysis techniques.

Chapter 3 - Methodology: Describes the research methodology, including UAV wing design and modelling, numerical simulation setup, and analysis procedures.

Chapter 4 - Results and Discussion: Presents and discusses the results of the numerical analyses, comparing the performance of aluminium and composite wing configurations.

Chapter 5 - Conclusions and Recommendations: Summarizes key findings, highlights the potential of composite materials in UAV wing design, and provides recommendations for future research.



2. LITERATURE REVIEW

The challenges of design and aerodynamics were addressed in a previous study in a high-altitude, fixed-wing mini UAV. The choice of suitable airfoils was also stressed when flying at high levels thus indicating that wing loading is primarily affected by factors other than changes in air density. It was found that the UAV performance was quite unstable when used under conditions different from what it was designed to operate, for example, at sea level, due to changes in lift and drag. The research also highlighted the importance of considering the lower air density and low temperature in the design of the airframe and subsystems of UVA during high altitudes. The operational condition is that the Reynolds number should be confined in a particular range for aerodynamic efficiency. Wind tunnel tests were performed on a prototype of the UAV to validate the theoretical predictions of aerodynamic performance and the ability of the UAV to remain stable and endure in various flight conditions. This research contributes to the understanding of particular aerodynamic problems that have to be addressed when designing UAVs for flight at high altitudes and provides a lot of related data for future work in this area [4].

In the previous study, a nonlinear dynamic model was developed for a fixed wing unmanned aerial vehicle (UAV) that was the Wulung UAV, to improve its control systems for different flight conditions. This model, based on the strict-feedback differential equations aimed to provide a precise simulation of the UAV's flight dynamics, which would enable the design of an adaptive control system. The study validated the model using simulations that closely matched actual flight data, showing its capability of predicting the UAV behaviour in various altitudes and airspeeds. This seminal piece of research sets a course for future developments of UAV control systems, emphasizing the critical role of nonlinear models in obtaining safe and reliable flight operations [5] .

In past research, examination was made on integration of smart material actuators for morphing wing applications for the purpose of maximizing aerodynamic efficiency. The study emphasized the importance of smart materials like Shape Memory Alloys (SMA) in correctable capacity of wing sections, and eventually increasing the aircraft performance within a range of flight conditions. Particularly, the study investigated the aerodynamic coefficients of an image-based model of a NACA 4412 airfoil at different angles of attack in both extended (morphed) and un-extended (un-morphed) configurations of wings. Results

showed a gain in aerodynamic behavior by elongation the wing part, with changes in the aspect ratio at various angles of attack [6].

To improve the aerodynamic efficiency of fixed-wing Unmanned Aerial Vehicles (UAVs), a study was conducted, and it concentrated on the structural design and optimization of the aircraft's wing. Wings play a critical role in determining the overall profitability of an aeroplane. Therefore, the research carefully analyzed different wing configurations, eventually deciding on a beam-type design for its unbeatable combination of lightweight structure and performance under operational conditions. This thorough analysis comprised a disciplined design sequence, which started by choosing an airfoil from reputable libraries that were well established and moved to a detailed review of structural choices. The selected beam-type wing was then optimized through a series of weight reductions that did not compromise the strength, stiffness, and durability necessary for long-endurance UAV flights. Crucial for this operation was the application of sophisticated computational tools such as finite element software for stress and strain analysis and CAD software for more accurate 3D modelling of the improved wing structure. The results of this study offer a systematic method of wing design and bring a contribution to general aerospace engineering in a framework which allows the developing more efficient and longer-flying UAVs [7].

In previous research, a novel solution was proposed to modify the flexibility inside an unmanned aerial vehicle (UAVs) wing structure, calling nature as an inspiration. This approach requires changing the inner structure of the wing to coerce its form under flight conditions to enhance aerodynamic character. One of the key findings is that the flexibility of a wing can be adjusted to substantially improve lift and endurance performance. The research employed advanced simulations to show how these alterations could result in more effective UAV performance, mirroring the efficiency of bats and insects. Efforts in the future will concentrate on the improvement of this innovative design idea used in the development of UAVs [8].

In one of the previous research, a detailed investigation was made on the aerodynamic behaviour of flapping wings of micro aerial vehicles (MAVs) under ultra-low Re number turbulent flow conditions. Computational fluid dynamics (CFD) was used by the study to model the flapping wings motion with emphasis on the NACA0012 and S1223 airfoil designs. This research has shown the intricate fluid-structure interaction (FSI) that

accompany wing flapping, the flowpath changes caused and as a result, forces generated aerodynamically. Finite Element Analysis (FEA) was employed to simulate the fluid flow and the coupling with the wing structure utilizing a direct numerical simulation approach. The aeroplane behaviour of both airfoils was studied under turbulent flow conditions by examining time dependent and FSI turbulence models to know how they influence lift and drag forces. The findings of the study showed that the flapping pattern results in wake modification of the wing, closely resembling the von Kármán vortex street. This trend was observed at all flapping rates indicating that the movement of the wing can greatly influence its aerodynamic performance by changing the flow separation behaviour. In addition, the findings provided knowledge on the best wing configurations and actuation systems that could be used in the flight controllers that would make MAV operate optimally at low Reynolds numbers. The results could be used as useful recommendations for developing more efficient flapping flight systems for UAVs, hence, improving the operational potential of these systems in such applications as environmental monitoring, aerial inspection, and search and rescue missions [9].

In a research study on Micro Aerial Vehicles (MAVs) at low Reynolds numbers, Fluid-Structure Interaction (FSI) simulations were employed to study the aerodynamic forces acting on flapping wings. An investigation was carried out on the flow dynamics around NACA0012 and S1223 airfoils, and the effect of the flapping motion and angle of attack on lift and drag forces was emphasized. Such research highlights the intricacy of aerodynamic effects within a low Reynolds number environment and offers guidance for improving the design of MAVs using bioinspired flapping mechanisms [10].

A past study involved the creation and validation of flight models of UX-6 fixed-wing Unmanned Aerial Vehicles (UAV) using both analytical and empirical approaches. Datcom+ Pro software was used to develop the analytical model through the given aircraft geometry data, while the empirical model was obtained from flight data through system identification. These models conducted in longitudinal and lateral flight modes showed that five parameters of the analytical model had similar features to the empirical model, pointing to a satisfactory representation of the flight dynamics of the UAV. This study is critical for improving UAV control systems and demonstrating the power of a hybrid of analytical and empirical modelling approaches for UAV design and optimization [11].

In one previous research, the one-way fluid-material interaction on plunging NACA-2412 modelled UAV wing was investigated. Both experimental and computational analysis were employed in the study to investigate the static aeroelastic responses of the UAV wings under a variety of aerodynamic loadings, at different Reynolds numbers, and angles of attacks. Wing deflections of the UAV were measured in the wind tunnel, mounted on a cantilever setup with a single degree of freedom, demonstrating what aerodynamic loading did to its structure. Afterwards, the ANSYS Workbench solid structural analysis tool was used for a comparison of the calculated data and the experimentally derived results. The study showed a large change in wing deflection resulting from fluid loading, with deflections ranging from 30% to 60% at different Reynolds numbers and angles of attack. This study emphasizes the necessity of including the fluid-structure interaction (FSI) analysis in UAV wing design for the improvement of aerodynamic performance and UAV standards [12].

One of the problems of forecasting the fatigue life of the fixed-wing unmanned aerial vehicle (UAV) engines under varying stress conditions in past research was solved using grey forecasting models. Such encapsulation restricts ventilation and causes thermal stress of engine degradation, which is a form of change of heat release characteristics. This state not only reduces the life of the engine but also induces premature failure. Applying grey forecasting models to degradation data of engine power across predefined reliable life hours, the study revealed under typical operating conditions, engine power would drop to a critical threshold after 100 hours. Nevertheless, under stressed environments, this life span was significantly reduced to 70 hours. The study demonstrates the suitability of grey forecasting for the prediction of mechanical degradation and possible premature failures with high precision especially in cases where data is limited [13].

An extensive study was carried out in earlier work to improve the aerodynamic modelling for parafoil systems flight dynamics simulation via fluid-structure interaction (FSI). This research was set to computationally obtain the aerodynamic attributes of the parafoils in place of expensive and less repeatable testing methods. Given the complexity of the nonlinear fluid-structure interaction between the flexible material of the parafoil and the surrounding flow field, this study set out to establish an accurate dynamic model by performing FSI simulations. The emphasis was especially put on the assessment of the aerodynamic performance of the full-size canopy with stabilizers for improvement of control. The novelty of the study was emphasized by the integration of strong coupling FSI

simulations using incompressible computational fluid dynamics techniques. The research further provided a database for the aerodynamic coefficients based on high-fidelity lift and drag force measurements, which was accomplished by conducting investigations of the effects of canopy inflation and trailing edge deflections on the performance of the vehicle. Following, the proper six-degree-of-freedom dynamic model of the parafoil system was developed, taking as input the estimated coefficients. Conducted simulations confirmed the model's dynamic stability and tracking effectiveness in comparison with airdrop testing data and showed that the model accurately predicts flight behaviour of parafoil systems [14].

The aerodynamic modelling for flight dynamics simulation of a parafoil system through fluid-structure interaction (FSI) was subjected to in a previous paper. The goal of this study was to obtain aerodynamic parameters of parafoils instead of standard experimental tool, considering the nonlinear effect of deformation of parafoil under airflow. The study sought to develop an accurate model of dynamic behaviour of parafoils under various flight conditions by means of FSI simulations. The emphasis was on assessment of the aerodynamics efficiency of the full-scale canopy with stabilizers in attaining control during the flight. By using incompressible computational fluid dynamics approaches, the research has provided an original understanding of the influence of canopy inflation and trailing edge deflections on aerodynamic performance. A database of aerodynamic coefficients was created with the aid of lift and drag force measurements, and as a result, an improved six-degree-of-freedom dynamic model of the parafoil system was implemented. The simulations of this model established its stability and effectiveness in trajectory tracking that matched closely with empirical airdrop test data, thus, highlighting this model's likelihood to accurately predict flight behaviors of parafoil systems [15].

A recent study looked into the fluid-structure interactions and aeroacoustic coupling effects of an airfoil with membranous suffocation to understand their contribution to low Reynolds number airfoil aerodynamics and noise minimization. The research used the direct aeroacoustic simulations to analyze what impact on aeroacoustic features different configurations of single and dual membranes had compared to a baseline rigid airfoil. A study showed that the manifestation of membranes, especially the paired membrane setup, markedly decrease airfoil self-noise but did not affect aerodynamic efficiency. This was realized by the distortion of upstream propagating acoustic waves by the displacement of the membrane thus, decreasing the coherence among pressure and velocity signals. Study

provides perspectives on exploiting fluid-structure interactions for noise control in airfoil design, demonstrating the ability of double membranes to achieve a marked reduction of tonal noise [16].

A previous investigation was carried out on the reconfiguration and analysis of a composite wing of a tail sitter (VTOL) UAV to improve performance through weight saving. The study exploited composite materials which are well-known for reducing aircraft structure weight by 30-50% while enabling strength and stiffness properties to be tailored via multiple ply configurations. Numerical analysis was done for comparisons of traditional aluminum frames and configurations using CFRP and GFRP composites with changes in spar numbers. Using the Finite Element Method, the strength and the stiffness of the UAV wing under span-wise lift distributions were considered, demonstrating that composite wings, particularly with CFRP, had a little deformation and better performance than the aluminum wings. The use of composite materials allowed to reduce the weight by 44.17% and preserved, if not improved, the wing's strength. This study emphasizes the paramount place of composites materials in the design of wings of UAV with VTOL configurations, which require high stiffness-to-weight ratio, necessary for carrying considerable loads [17].

In a previous research, fluid-structure interaction (FSI) simulations were used for evaluating the aerodynamic behavior and structural responses of composite laminate wing skins under aerodynamic loading. The study compared the structural responses of UAV wings with composite wing skins with honeycomb and without honeycomb denoted as CWS and CWSwH respectively. Using CFD for aerodynamic loading analysis and FEA for structural response, the investigation proved that the integration of honeycomb in composite laminates (CWSwH) reduced deformation, signifying improved structural integrity relative to the non-honeycomb configuration (CWS). The findings emphasized the importance of honeycomb structures in enhancing the durability and aerodynamic performance of UAV wings, thus providing a useful path for the optimization of UAV design through advanced simulation techniques [18].

In the previous study, a brand-new large-scale, serviceable, steady multi-dimensional morphing wing skeleton (MWS) mechanism was introduced, which was made up the modular bilateral triangular pyramid (BTP) units. This allows for a Lockable Morphing Unit (LMU) that provides span-wise bending variations through bending, twisting and sweeping,

hence, enhancing the overall aerodynamic performance at different flight states. The method of Denavit-Hartenberg coordinates was applied to analyze the kinematics of the MWS mechanism followed by the motion influence coefficient method which resulted in theoretical models describing kinematic properties in all morphing modes. The following kinematic simulation models were created for the three morphing configurations, thereby confirming the accuracy of the kinematic theoretical models. A two-way fluid-structure interaction (FSI) study showed how the flexible skin and skeletal mechanism is affected by the aerodynamic load and how structural deformation affects the aerodynamic characteristics. Morphing wing configurations, especially in the case of the swept state, have a significant influence on the out-plane bearing capacity of the flexible skin, and some deformations are beneficial for the aerodynamics performance. These concepts provide an efficient theoretical basis for the implementation and improvement of the MWS mechanism in morphing wings [19].

A past research comprehensively explored the aerodynamic performance and structural dynamics of flapping-wing rotorcraft, taking into account the effects of stiffness, through fluid-structure interaction (FSI) analysis. This study emphasized the importance of wing stiffness in increasing lift and improving the aerodynamic performance of flapping-wing rotorcrafts (FWRs). Using a simplified structural model-based computational FSI approach a significant improvement in lift force up to 36.2% was achieved through strategic changes of wing stiffness. The results of the study have substantiated the proposed computational approach in terms of experimental data, which has thereby been proven to be rather efficient in predicting the intricate interactions of the aerodynamic forces and the wing deformations. In addition, the investigation covered the aerodynamic flow features and pointed out the connection of wing deformation modes with lift and glide dynamics. The results of this research provide inputs to the general knowledge of the design and optimization of FWR, thus, an attractive field for prospective UAV technology developments [20].

In earlier studies, the development and manufacturing processes of a fixed-wing Unmanned Aerial Vehicle (UAV) were extensively investigated and off course, the procedural approach from ideation to a detailed design and analysis. Using computational tools and numerical analyses, including Fluid-Structure Interaction (FSI) and Computational Fluid Dynamics (CFD), the research carefully analyzed the UAV's aerodynamic performance and structural integrity. Due to a focus on material selection and fabrication methods, an optimal balance

of weight and durability was attained for UAV. All tests during the comprehensive testing phase confirmed the structural and aerodynamic models for efficiency of flight of the UAV. This study addresses the subtle interplay between ultimate design and practical usability in respect to UAVs development [21].

A recent study proposed an optimization method for a multi-component airfoil of a fixed-wing airborne wind energy system. This method customized the airfoil's design to fit the specific needs of both the generation and return phases of the kite's operation, with the ground-based drum-generator module. By first optimizing the airfoil for production phase and then modifying the flap settings for return phase, a complete solution was developed to improve power output. The optimization was carried out by NSGA-II genetic algorithm and fast aerodynamic solver that upon finding the ideal shape further validated it through CFD RANS simulations in OpenFOAM. The ultimate design demonstrated acceptable aerodynamic performance at both operational stages, whereby lift coefficient results corresponded closely with theoretical forecasts. This revolutionary optimization approach highlights the possibility of advanced design solutions to enhance the efficiency and the reliability of the airborne wind energy systems [22].

High-fidelity fluid-structure interaction simulations were used to perform a comprehensive study of wing deformation of an Airborne Wind Energy (AWE) system during crosswind flight in recent research. The aim of the study was to detail the complexities of unsteady aerodynamic interactions with the dynamic system, which is a crucial element of scalable AWE systems development. Using a partitioned and explicit manner, the study associated a computational structural mechanics model of the wing structure with a computational fluid dynamics model of the wing's aerodynamics. The integrated simulation methodology enabled the rigorous evaluation of a wind deflection effect on AWE system performance during crosswind maneuvers. The principal reveal was that wing deformation improves the symmetry of spanwise loading, a fact that could be quite useful in future AWE system designs in the efforts to increase energy effectiveness. This research not only pushes the boundary of understanding the operational dynamics of AWE systems but also provides a methodological basis for using high-fidelity simulations in the design and optimisation of these emerging energy technologies [23].

In a previous paper, a unique hierarchical coupling approach was used to evaluate the flight performance of polymer micromachined flapping-wing nano air vehicles (FWNAVs) which concentrated on the relationship between structural dynamics and fluid-structure interactions. The methodology helped to decompose the complex FWNAV system into subsystems for in-depth study aimed at refining flight performance by strategic changes to wing skin thickness and stiffness. Major outcomes illustrated an opportunity to apply fluid-structure interaction analysis to improve FWNAV aerodynamic efficacy and structural resilience. The current work presents a significant contribution to the development and optimization of FWNAVs, pointing out the critical role of computational simulation in improving the efficiency and reliability of unmanned aerial vehicles [24].

In arecent research, a fluid-structure interaction simulation was used to forecast the effectiveness of performance and serves as a design optimization tool for parafoils. Such approach was designed to provide true representation of forces and responses of parafoils in different flight conditions. Using a two-way coupled fluid-structure interaction approach, the study described the incorporation of nonlinear finite element techniques for the canopy fabric model with sophisticated fluid dynamics solvers. It gave the simulation a possibility to depict the real performance of parafoils under aerodynamic loadings, giving a more accurate background for improvements. The simulations centered on full-scale parafoil canopies to study their equilibrium shapes and the associated flow fields and to improve design confidence. The results illustrated that the canopy inflation and structural adaptation greatly affected the aerodynamic efficiency and thus provided valuable information for the optimization of parafoil systems to improve the flight performance. This research represents a key move to using high-fidelity simulation tools in the implementation as well as eliminating the need for the application of empirical tests as the part of the parafoil design process [25].

In earlier research, the behaviour of an adaptive NACA aerofoil using Shape Memory Alloys (SMAs) was studied regarding fluid-structure interaction with heat transfer effects. The purpose of the research was to investigate the effects of thermal inputs, which were conditioned by the operational requirements of the aerofoil, on its shape deformation and, hence, on its aerodynamic characteristics. Using a truly coupled simulation model that includes the structural, fluid flow, and thermal behaviours, the study demonstrated that the adaptability of the aerofoil substantially influences its lift-to-drag ratio. This flexibility,

facilitated by the heat-induced activation of the SMAs, permits the aerofoil to change its geometry to correspond with the flight conditions changes and thus maximize the aircraft efficiency and economic use of fuel. The results of this study reveal the possibility of utilizing thermally activated adaptive shape shifting aerofoils to improve the aerodynamic efficiency of aircraft which is an important move in the direction of more flexible and efficient flight systems design [26].

In a recent research, the emphasis was on designing a computational framework for the study of fluid-structure interaction (FSI) effects on passive feathering and cambering in flapping insect wings. This study is intended to address passive aerodynamic effects of the inherent elasticity of the wings under flow forces using comprehensive numerical approach for parametric studies. The framework provided a completely parallelized solution method to deal with monolithic FSI equation systems, assuring stability numerically under a plethora of conditions, even substantial elastic deformations and body motions. Further, a novel structural mechanics model for simulating the complex flapping dynamics of insect wings was developed using pixel modeling to drastically reduce computational complexity. The evaluation of this framework against established benchmarks confirmed its effectiveness in accurately reproducing the complex relationship between wing deformations and aerodynamic forces, thus offering useful data for the design and optimization of bio-inspired flapping wing systems [27].

In a previous study, the aerodynamic performance of supercritical wings was investigated with computational fluid dynamics (CFD), with the lift-to-drag ratio being the main parameter of interest. By comparing the supercritical wing to the flat wing under identical conditions, it was observed that the aerodynamic efficiency of the supercritical wing is higher, especially during the cruising stages. For instance, it was established that under normal cruise conditions, the supercritical wing lift-to-drag ratio takes a significant increase of 1.869 times more than that of a flat wing. This improvement emphasizes the capacity of supercritical wings in enhancing the performance of aircraft making them an essential design feature of contemporary airlines. The application of CFD for the analysis in the study is an important part of further development and tests of aerodynamics of supercritical wings [28].

A past research employed the computational fluid dynamics (CFD) simulations to analyze the effects of ski-jump decks on the take-off zone flow field of aircraft carriers. The objective

of the research was to determine the effects of ski-jump deck configurations on the aerodynamic characteristics of carrier-based aircraft at takeoff. Through simulation of different scenarios, it was found that ski-jump deck greatly influences the airflow around the take-off zone, significantly affecting the engine intake of the carrier-based aircraft because of body-shedding vortices produced on the sides of the bow. These results highlight the role of design of ski-jump deck in improving the aircraft take-off performance and thereby offer useful inputs for the optimization of the aircraft carrier configurations. The study provides greater insight into the intricate phenomena underpinning the interaction between aircraft carrier decks and airflow parameters on carrier launched aircraft takeoff and thereby, contributes to the development of naval aviation technology [29].

In an earlier research, a combination of fluid structure interaction (FSI) simulations with flexible multibody dynamics and a modified unsteady vortex lattice method was used to study the effects of flexibility on flapping aquatic wings that were known to mimic the movement of a manta ray. This study sought to improve the design of such wings, which have attracted attention in submarine vehicles because of the continuous and low-cavitation propulsion method they offer. Using a novel simulation framework, the research investigated the effects of wing stiffness and flapping motion on propulsion efficiency and thrust generation. It showed that the change of flexibility in the wings can dramatically improve the propulsive efficiency even though the trade-off in thrust coefficient is detected. The presented method offers a holistic approach to the prediction of intricate relations between the wing structural dynamics and the surrounding fluid of the wing, and hence, may provide guidance for designing more successful and efficient flapping-wing vehicles [30].

In a prior study explored an effect of camber morphing on the aeroelastic and aerodynamic performance of wings by implementing a novel shape memory alloy actuator for trailing edge deformation. The research used computational fluid dynamics (CFD) as well as wind tunnel experiments to investigate the aerodynamic forces of camber morphing wings with and without trailing edge deformation. The study showed the strength of lift that the downward deflection of the trailing edge brought on the wing by changing the velocity flow over the lower wing surface, relocating the position of the shock wave forward, therefore eliminating the negative pressure zone on the upper surface and adding pressure on the lower surface. This fluid-structure interaction (FSI) research presents a new principle of rear edge

deformation implementation, giving large mass of data for the design of camber morphing wings and making our understanding of their aerodynamic performance enhanced [31], [32].

A comprehensive fluid-structure interaction analysis was recently conducted in a paper to investigate the aerodynamic performance of a camber morphing wing. The study employed computational fluid dynamics (CFD) together with wind tunnel tests to assess the aerodynamic forces acting on the wing with different levels of camber morphing, especially in relation to trailing edge deformation. The results showed that the negative deflection of the trailing edge increased lift by changing flow pattern over the wing and moving the shock wave forward that reduced the negative pressure on the upper surface and increased the pressure on the lower surface. This study emphasizes the need to include fluid-structure interaction analyses in the morphing wing design, which gives vital details on their aerodynamic behavior optimization [32].

Previously, a scientific paper was devoted to lateral-directional aerodynamic optimization of a tandem wing Unmanned Aerial Vehicle (UAV) by means of computational fluid dynamics (CFD) analyses, aimed at increasing the lift-to-drag ratio and providing stability. In the beginning, the UAV was tailored for symmetrical flight situations which emphasized that both wings generated the positive lift, wherein the front wing stalled first to keep control and stability. The optimization process comprised of removing the lower vertical tail, using a negative dihedral on the front wing, and incorporating four inverted blended winglets, resulting in a model known as TW V14. This version of the model contributed greatly to the improvement of the side and directional stability features in such a way that the longitudinal performance was not compromised. The research brings the role of utilization of CFD analyses in aerodynamic optimization, especially for UAVs with complex configurations such as tandem wings, and emphasizes on the compromise between aerodynamic efficiency and stability in UAV design [33].

An earlier study introduced a unified fluid-structure interaction (FSI) modeling framework for assessing the aerodynamic optimization of a tandem wing UAV using computational fluid dynamics (CFD) techniques. The study was aimed to enhance aerodynamic efficiency of the UAV with special reference to the lift-to-drag ratio and flight stability. After the CFD analyses, the UAV was optimized under a condition of symmetrical flight, where both wings create positive lift with the front wing designed to stall first for control and stability. The

optimization process resulted in the creation of the TW V14 version that included a reduction of the lower vertical tail, application of the negative dihedral to the front wing and installation of four inverted blended winglets. This setup drastically improved lateral and directional control without sacrificing longitudinal deterioration. The results demonstrate the use of CFD analyses for aerodynamic optimization in the context of UAVs with complex configurations such as tandem wings, which emphasizes the necessity of achieving a trade-off between aerodynamic efficiency and stability in UAV design [34].

In a recent study, a comprehensive design process was executed for a fixed-wing Blended-Wing-Body (BWB) Unmanned Aerial Vehicle (UAV) intended to operate within a Cooperative-Intelligent Transport System (C-ITS). With the help of Carbon Fiber Reinforced Polymers (CFRPs) and Additively Manufactured materials, the study solved the problem of creating a lightweight but strong UAV structure, that would be able to survive the operational requirements of highway traffic monitoring. Finite Element (FE) simulations were a key tool in structural component sizing, which guaranteed the structural integrity of the UAV under different flight conditions. The iterative design process between aerodynamic and structural teams enabled the achievement of the ideal balance between performance, effectiveness, and durability. The successful production and testing of the UAV prototype revealed the power of combining current materials with FE analysis in UAV design, opening up new opportunities in C-ITS applications [35].

In one of the previous papers, an investigation of the structural analysis of wings of the Unmanned Aircraft Vehicle (UAV) under wind gust conditions was done by fluid-structure interaction (FSI) analysis employing computational fluid dynamics (CFD) and finite element analysis (FEA). A gust of wind, replicated as an abrupt airspeed increase, was observed to greatly influence the lift and drag forces on the wings while lift substantially increased in the gust condition. The aerodynamic loads obtained from the CFD simulations were imposed on a structural model in ANSYS MECHANICAL in order to investigate the structural response of the wings. The investigation showed that the maximum stress was located on the slender part connecting the spar and shell of the wing and the stress was way below the critical value even under gust condition. The combination of CFD and FEA integrated in this research gave a complete approach for predicting structural integrity of UAV wings and the capability to withstand the larger loading without safety compromise was demonstrated [36].

In a previous research, numerical simulations were used to explore structural and fluid dynamics to enhance aerodynamic performance, particularly in the aspect of bio-inspired unmanned aerial vehicle (UAV) wing design and the streamlined body with leading edge (LE) erode due to damage. The study used computational fluid dynamics (CFD) to investigate the conformal tailoring of passively induced airfoil shapes for slender UAV wings and assessed the aerodynamic characteristics of wind turbine blade airfoils with idealized leading edge damage patterns that mimicked erosion effects. The research provided the example of the advantages flexible, passively deforming wings have for the UAV wings, to make it to fly longer, use less power and possess better stability. Using some computational tools of various accuracy and fidelity, the research was aimed at optimizing the distribution of the wing flexibility of UAV to make these improvements. The study demonstrated that erosion was the most significant leading edge feature that affects aerodynamic performance and further work on fluid dynamics is required to understand erosion effects and to direct design optimisation. The applications areas of both aimed to develop basic understanding by use of computationally simulations as a basis of driving design optimisations aimed at performance improvement. One study showed that flexibility tailoring was vital in UAV wings; this helped maximize the aerodynamic advantages while another study discussed how leading edge erosion affected the efficiency of wind turbine blades [37].

In one of the previous works, Fluid-Structure Interaction (FSI) analysis was used to investigate the influence of mass distribution on the wing flutter. One of the main aims was to analyze how modifying the center of gravity influences in a flutter-related manner speed characteristics of wing flutter. The study included placing point masses at different locations across the wing and observing the change in aeroelastic response. This study used an integrated approach which coupled both structural dynamics and computational fluid dynamics (CFD) to provide a more realistic simulation of the actual world scenarios. Validation of the analytical technique was done by comparison with the experimental results of the AGARD 445.6 wing flutter test which showed a good match. The results of this study are critical for the layout and optimization of wings, providing details on flutter management using targeted mass distribution. This makes a major contribution to improving the safety and reliability of aircraft in aeroelastic stability [38].

In previous research, the design of a UAV wing was based on the use of eco materials. Skywalker X8 model was the focal point. The skin of the wing box is polypropylene, while its honeycomb structure is made of balsa wood with the goal of light weight and structural efficiency. Analytical computer simulations provided for the correctness of the materials selected which guarantees structural strength and aerodynamic performance within an acceptable stress range under various flight conditions. An investigation of a Gurney flap aimed at aerodynamic improvement resulted in little performance gain. This research emphasizes the possibility of incorporating ‘greener’ technology into the designs of UAVs, recognizing the crucial location of material choice and structural designs in the advancement of UAVs efficiency and sustainability [39].

In one of the previous studies, a thorough Computational Fluid Dynamics (CFD) analysis was carried out on a fixed-wing Unmanned Aerial Vehicle (UAV) intended for reconnaissance use, emphasizing its aerodynamic stability and versatility for both civil and military uses. The UAV characterised by a wingspan of 1.5 m and a fuselage length of 1.135 m was simulated for its flight performance, including take-off, cruise and landing phases. The CFD simulation results validated that the design provides greater velocity over the upper surface of the wing, which leads to efficient lift production, ensuring stable flight characteristics in the simulated environment. Moreover, the study showed that the UAV design, particularly including advanced materials and communication systems, allows real time video feed for surveillance, and is not limited by distance due to the internet based control system. This highlights the potential of the UAV in augmenting wide-area surveillance abilities, backed by CFD analysis confirming its aerodynamic solid and performance [40].

In the previous research, a unique fluid-structure interaction (FSI) environment was developed to evaluate the aerodynamic performance of flapping wings. This environment combines high-fidelity fluid dynamics and structural mechanics simulations to replicate the intricate movement and deformation of flapping wings, similar to those found in nature. The linking of the Computational Structural Mechanics (CSM) software Kratos Multiphysics with Computational Fluid Dynamics (CFD) software OpenFOAM was realized with the software CoCoNuT, which is based on IQNI method for the load and deformation interfacing. The concept was verified through a case study of an airfoil in heave motion, revealing large impact of wing flexibility on aerodynamic performance. The capacity of the

FSI solver to accurately model huge motions and deformations can provide information for creating more effective Flapping Wing Micro Air Vehicles (FWMAVs) by using flexible wings to utilize aerodynamic advantages [41].

In a previous study, Aero-Structural and Control stability analysis were conducted for a VTOL configured Hybrid Blended Wing Body based UAV, which was designed for surveillance, specifically for intruder inspections. The study, by incorporation of fluid-structure interaction (FSI) modeling, computational fluid dynamics (CFD), and control stability simulations, revealed the aerodynamic performance and stability of the UAV in vertical takeoff and landing (VTOL) operations. Stressing the enhancing surveillance capability of the UAV, the analysis underlined the role of aerodynamic design for the stable flight and efficient maneuverability. The results indicate that UAVs, which have been optimized for the stability of the aerostructural features with proper control stability systems, would increase the efficiency of surveillance applications. This work contributes to the field of UAV design, especially for VTOL configurations, by showing that aero-dynamic and control stability studies are important in the development of UAVs for complex missions [42].

In recent research the aerodynamic effects of a three-blade propeller in multirotor UAV applications were studied through the use of Computational Fluid Dynamics (CFD) modeling techniques. The attention was directed to the comparison of Multiple Reference Frame (MRF) and Sliding Mesh (SM) methods regarding their accuracy in describing the operational dynamics of the propeller at various rotational speeds and Reynolds numbers. These methods were tested with the use of experimental data found in the literature, demonstrating fidelity and computational efficiency of each method. Additionally, Richardson's extrapolation method was used in the study to measure the uncertainty that comes with computational modeling. This study highlights the importance of precise CFD modeling in the initial design stages of UAVs, especially in improving the aerodynamic performance of the propeller, which is critical in increasing the UAV's flight efficiency and control characteristics [43].

In a recent paper, an optimal and implementable parametric form of an aerodynamic model for a delta-wing UAV had been found for model-based navigation. The study proposed a hybrid method which involved wind tunnel tests performed in open atmosphere along with

the analysis of flight research data by use of filter error method. This technique increased the ability to identify aerodynamic coefficients of UAV under time limitation. The process included using Latin Hypercube Sampling for the experimental design, selection of candidate models through stepwise regression, determining numerical values of the model coefficients experimentally, and calibration with real flight data. The experiment showed that the model-based navigation using the suggested aerodynamic models decreased positioning errors significantly compared to traditional navigation approaches during GNSS outages in four test flights. This proves the usefulness of the proposed aerodynamic model in improving the navigating ability of UAVs when GNSS signals are not presented. The research highlights the significance of incorporating fluid-structure interaction studies in the development of morphing wings, giving knowledge on the optimization of UAV systems for better flight performance and efficiency [44].

3. METHODOLOGY

This chapter will introduce the basic scientific principles and theories that underlie a range of number counts and simulations, which will be conducted in this study. At first, the basics of aerodynamics and computational fluid dynamics will be given, including the governing equations and factors like boundary layer and forces acting on objects in an aerodynamic field. Subsequently, the theory of fluid-structure interaction, which represents the main focus of the study, will be introduced, with explanations of the two primary approaches: two-way fluid-structure interaction and one-way fluid structure interaction.

In addition, the finite element method, one of the most important tools in the complex engineering and mathematical analysis, will be discussed, explaining its steps and applications in different areas. Moreover, a review of composite materials, classifying them and several failure criteria applied in their analysis will be given.

Lastly, the last part of this chapter deals with the design and numerical simulation of a particular Unmanned Aerial Vehicle (UAV) wing, the AAI Shadow-200 RQ-7. The wing design details will be provided with the usage of some software, like SolidWorks, with the list of settings and steps for the numerical simulation in the ANSYS software. Various analyses such as computational fluid dynamics, fluid-structure interaction, and natural frequency analyses will be done on aluminum wing and different composites to be able to compare their performance.

3.1 AERODYNAMICS

3.1.1 Introduction

The science of aerodynamics shall be determined by the resultant forces and change of shape that an object passes through whenever air is present. It is the area dedicated to functions meeting every expectancy, across a broad spectrum of applications - flow over a wing of an aircraft, flow in an engine of a vehicle and prediction of weather patterns. As its other main branch dealing with air dynamics demonstrates, the effects air has on objects that are exposed to it, especially in terms of air around the objects, is given more focus in the class. Fundamentally, aerodynamics is an area of science with the objective of investigating how objects behave when they are in contact with air and why the forces acting on objects differ due to such interactions. The information conveyed by these measurements, however, covers

opportunities to develop and improve vehicles, buildings, and engineering systems in general, by improving their performance, efficiency, and security. Foundations of aerodynamics is based on the fundamental laws of fluid dynamics which represent the way in how air, regarded as a medium, behaves with regards to solid properties. Aerodynamics engineers borrow from the principles of aerostatics in their efforts to forecast aerodynamic forces of lift, drag, and moments that act on various shapes, namely airfoils and wings but also on aircraft as a whole and even ground vehicles. This is a key concern for aids design and operation; it allows aircraft to generate lift and be stable while at the same time resisting little or no hampering. Besides aerodynamics, it is key to evaluate the performance development of the sport equipment wind turbines too in the environmental studies and disaster warnings strategies. From an aerodynamic perspective, there is theoretical zooming into subsequent classes based on how fast the object and sound fly in both levels, including subsonic, transonic, supersonic, and hypersonic aerodynamics. All categories divided into separate courses, which, as a result, have unique sets of problems and patterns that cannot be handled with one common approach or technique. Conventional aerodynamics utilizes experimental testing, analog visualizations as well as digital simulations in the process of modeling air flow around objects. By adopting a multi-disciplinary approach, the engineers are enabled to be more fruitful in designing and building of the air vehicles to achieve the most efficiency of their usage, minimize energy consumption and get to the bottom of the complex aerodynamic problems [45].

3.1.2 Concepts

a. Boundary layer

The boundary layer is a thin layer of fluid in direct contact with a solid surface where the role of viscosity (internal resistance of the fluid to flow) is quite essential. Inside this layer, the fluid velocity goes from zero at the surface (because of the no-slip condition) to nearly the free stream velocity outside the boundary layer. Understanding this idea is crucial for characterizing the behaviours of the diverse forces, mainly drag forces, to which the equivalent forces on the objects that move through a fluid are subjected [46].

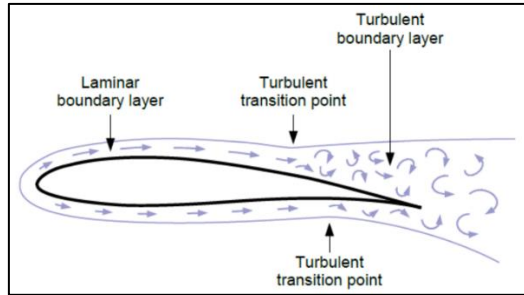


Figure 3.1: Boundary Layer on Fixed Wing of Aircraft [47].

b. Drag forces and coefficient of drag.

- i. Friction Drag: This is caused by shear stress (i.e., force per unit area) acting on the object's surface in the flow direction. It is essential in slender bodies where the stream remains attached to the surface [46].
- ii. Pressure Drag is the difference in pressure between the front and rear ends of an object moving in a fluid. It is more prevalent in blunt objects where flow separation occurs, leaving a wake of low-pressure fluid behind the object [46].
- iii. Drag Coefficient The drag coefficient, which is a non-dimensional number, measures the drag or resistance of an object in a fluid environment. It is defined as [46]:

$$C_D = \frac{2F_d}{\rho v^2 A} \quad (3.1)$$

where, F_d is the drag force, ρ is the fluid density, v is the object's velocity with respect to the fluid, and A is the base area (for cars the frontal area, for wings the planform area etc.).

c. Lift effects on lifted bodies

Lift is the force perpendicular to the direction of movement through the air, essential for an aeroplane flight. Bodies to be lifted, such as aerofoils, are intended to optimize this force but minimize drag [46].

The form of an aerofoil determines the amount of lift it can produce. The lift force (L) is a function of the fluid density (ρ), and the lift coefficient (C_L), which varies with the angle of attack (α) [46]:

$$L = C_L \cdot \frac{1}{2} \rho v^2 A \quad (3.2)$$

The angle of attack is the angle between the airfoil's chord line (a straight line connecting its leading and trailing edges) and the oncoming airflow direction [46].

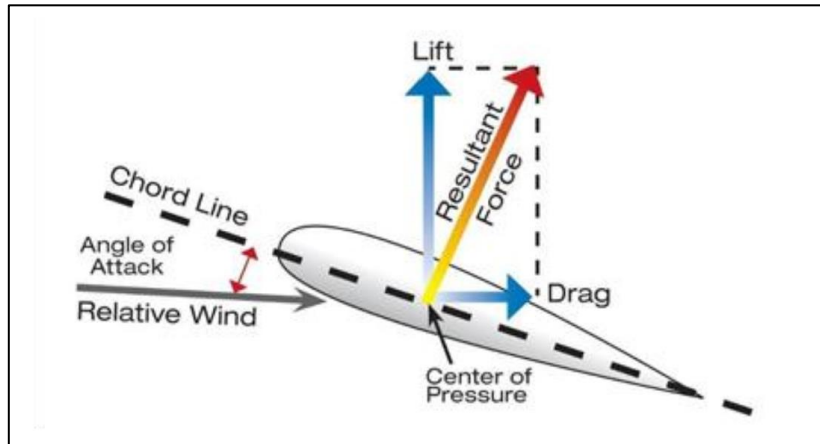


Figure 3.2: Different forces that Affect the Aircraft's Fixed Wing [48].

d. Stall and high lift devices

Stall happens when an airfoil surpasses the critical angle of attack, causing speed loss and drag gain to the point of the flow separation over the airfoil's upper surface. High-lift devices change the shape of an airfoil, enhancing the maximum lift coefficient, which makes taking off and landing at lesser speeds safe [46].

Stall is the term used to describe the leading edge of the curve, which results in a negative lift. The stall speed (V_{stall}) at which an aircraft begins to lose lift is determined by its weight (W), the gravitational constant (g), the air density (ρ), and the wing area (A): That is the horizontal line which is also known as the lift curve slope. Where the maximal value of the stall speed equals the certain given aircraft weight (W), gravitational constant (g), air density (ρ), and wing area (A) [46].

$$V_{stall} = \sqrt{\frac{2W}{\rho A C_{L_{max}}}} \quad (3.3)$$

3.2 COMPUTATIONAL FLUID DYNAMICS

3.2.1 Introduction

Computational fluid dynamics (CFD) is a part of fluid mechanics that is useful in practice for simulating multi-dimensional fluid flows using numerical methods and data structures. A computer model is given to the computer programs that make the required calculations to model the behaviour of an idealized fluid under the imposed boundary conditions. After

many years, CFD has become a well-known and indispensable instrument in academic or industrial applications, going through various industries, capable of providing detailed information on very complicated fluid flow phenomena that would be difficult or impossible to do with traditional models. The development and coming of CFD are persistent; the CFD market grows year by year at an impressive rate as most CFD tools are used to design and optimize products, from cars to aircraft along the road. On the one hand, user-friendly pro-commercial CFD software, as a new phenomenon, has made digital tools accessible to a greater community than ever before; on the other hand, to use them effectively and reliably, one has to have a good deal of theoretical knowledge within the area of fluid mechanics, which is the source of CFD. The uncharted frontier for studying fluid behaviour at scales and with accuracy levels beyond what is possible now is the combination of factual knowledge and computational venues. This opens new ways to study and use fluid motion in new and creative ways [49].

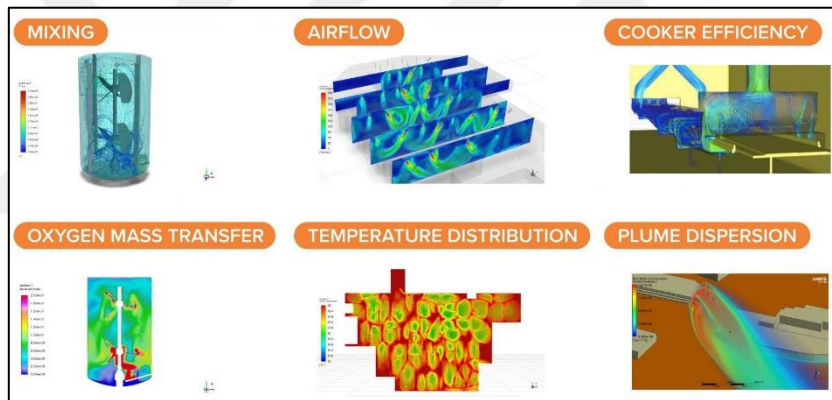


Figure 3.3: Some of CFD Applications in Different Fields [50].

3.2.2 Governing Equations

a. Continuity Equation

The Continuity Equation represents the conservation of mass in a fluid flow [51]:

$$\frac{\partial \rho}{\partial t} + \nabla \cdot (\rho \vec{v}) = 0 \quad (3.4)$$

where, ρ is the fluid density (mass/volume), indicating how much mass is contained within a unit volume of the fluid, \vec{v} is the flow velocity vector (distance/time), representing the speed and direction of the fluid movement, $\frac{\partial}{\partial t}$ denotes the partial derivative with respect to time, indicating how the density changes with time at a point, and ∇ symbolizes the

divergence operator, measuring the rate at which "mass" exits a volume at a point based on the velocity field.

b. Momentum Equation

$$\frac{\partial(\rho\vec{v})}{\partial t} + \nabla \cdot (\rho\vec{v}\vec{v}) = -\nabla p + \nabla \cdot \tau + \rho\vec{g} \quad (3.5)$$

where $\rho\vec{v}$: is momentum per unit volume, p is the pressure exerted at a point within the fluid (force/area), related to the force applied perpendicular to a surface, τ represents the viscous stress tensor, accounting for internal frictional forces within the fluid due to its viscosity, g is the gravitational acceleration vector (distance/time²), indicating the acceleration due to gravity, and The terms ∇p and $\nabla \cdot \tau$ corresponds to the spatial gradients of pressure and viscous stresses, respectively, showing how these quantities change from one point to another within the fluid.

c. Energy Equation

The Energy Equation, based on the first law of thermodynamics, describes the conservation of energy within the fluid:

$$\frac{\partial(\rho E)}{\partial t} + \nabla \cdot ((\rho E + p)\vec{v}) = \nabla \cdot (\vec{q} + \tau \cdot \vec{v}) \quad (3.6)$$

where, E is the total energy per unit mass, which includes internal, kinetic, and potential energies, \vec{q} is the heat flux vector (energy/(time. Area)), representing the rate at which heat energy is transferred per unit area, The term ρE denotes the energy per unit volume within the fluid, The expression $(\rho E + p)\vec{v}$ accounts for the convective transport of energy and the work done by pressure forces in moving the fluid, and the term $\tau \cdot \vec{v}$ represents the work done by viscous forces within the fluid.

3.3 FLUID STRUCTURE INTERACTION

3.3.1 Introduction

The Fluid-structure Interaction (FSI) is described as the mutual interaction between a deformable structure and the fluid flow (either internal or surrounding flow) where the pressure field of the fluid causes the structure deformations and, at the same time, the geometric domain of the fluid also updates itself considering the structural deformations. FSI is the key to the simulated liquid flow works of the mechanical structures whose

resistance to these forces is critical for the entire system. It can be classified into two main approaches: It can be classified into two main approaches [52]:

One-Way FSI: This method is characterized as the one that considers the accumulated deformations of the structural elements to be minimal and is not very influential on the current surrounding environment (fluids). This turned out to be because solutions of CFD (Computational Fluid Dynamics) and structure analysis can now be treated as two independent problems in which unidirectional data transfer between the fluid and structural domains is performed. The process employs the principle of specific stress transferor, which is the only form of pressure exerted by the fluid, to determine the structural response of the model. Often, this method is employed for small/minor alterations when the impact of structural changes on the fluid flow is unimportant and can be ignored [52].

Two-Way FSI: This, on the one hand, acknowledges the influence of fluid flow on structural response and structural response on flow. As a result of fluid pressure, the structure experiences deformations, developing a complex flow field that implicitly requires unidirectional data exchange between fluid and structural domains. The duo of domains need to be presented entirely, and transport of pressure from the CFD to structural analysis and a deformation correction of the data from structural to CFD analysis is being done at each iterative step until convergence to an acceptable outcome is achieved. This approach is imperative for engineering matters in which the mutual interaction of the fluid and structure may heavily influence the characteristics of the system, and, in this case, disregarding this mutual effect may lead to errors in predictions [52].

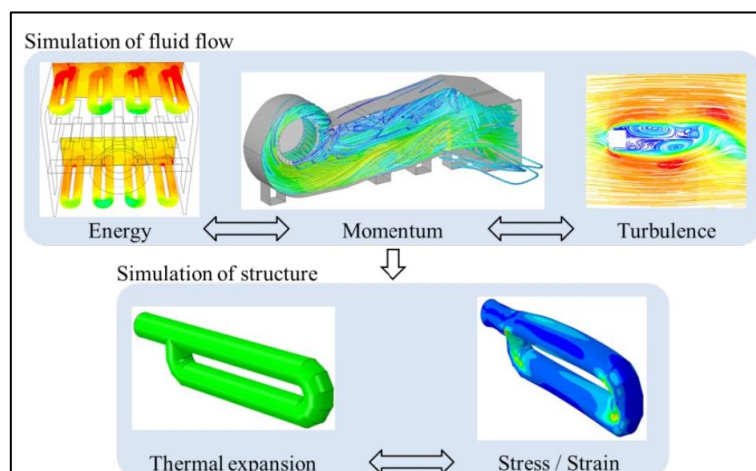


Figure 3.4: FSI Analysis Workflow [53].

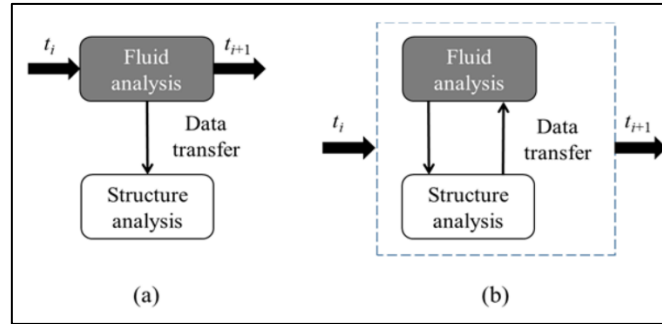


Figure 3.5: (a) One-Way and (b) Two-Way Interaction Approaches for Fluid-Structure Integration [52].

3.4 FINITE ELEMENT METHOD

3.4.1 Introduction

The finite element method (FEM) is a compelling numerical calculation method used to compute complicated problems in engineering, and mathematical physics, where analytical solutions are too complex or impractical to obtain. FEM splits massive systems into small, elementary sub-systems, wherein the solutions of the equations represent the approximations of the solutions of these sub-systems. This method is highly convenient for structural analysis, heat transfer, fluid dynamics, and electromagnetic potentials. It allows engineers and scientists to develop complicated geometry, a wide range of material properties, and boundary conditions with significant accuracy. The evolution of FEM has been much guided by computer innovation, the designs of which find a real-life application in the analysis of complicated systems with hundreds of thousands of elements and unknowns. The FEM technique extends various physical systems capable of mimicking stress distribution, convection matters, the flow of fluids and other critical physical aspects which are of high importance for engineering design and analysis. The Finite Element Analysis (FEA) absorbs the principles of FEM into their classic engineering problems, producing a detailed visualization of where structures bend or twist and the progression of stresses and displacements. FEM-matured FEA software packages help engineers predict their products' real-life behaviour effectively before running extensive and expensive tests. This allows us to explore innovation in numerous spheres by eliminating weak designs [54].

3.4.2 Finite Element Methods Steps

This method is structured into three critical phases: firstly, preprocessing takes away a lot of distractions and offers a solution, and finally, postprocessing brings accurate results [55].

a. Preprocessing Phase

Domain Discretization: Placing a solution decision into exact parts is done by dividing the solution's domain into more minor, finite elements that can be managed. It follows specific steps in the way of providing access to a computer model through which the desired domain of the problem is observed and so studies its behaviour under several conditions [55].

Shape Function Assumption: The shape function explains the correct behaviour of each element by describing an undulation in the deformation of an element. This function, which has a continuous form, compares the element's behaviour with the analysis's result. As a result, it enables us to proceed to the next step of the analysis [55].

Element Equation Development: The behaviour of a physics system or event system is explained, which enables the formulation of formulas for each element. Equations of the above equation type are particularly useful in the numerical calculations of these relationships between the nodes and the elements, which form the mesh [55].

System Assembly: Thing for these element equations before assembling them to the entire problem. It captures all the processes from formulation till the global stiffness matrix that is required to solve the complete [55].

Application of Conditions: The boundary conditions, initial conditions and loadings are added as part of the post-processing process during the model generation. This first level is the necessitated one through which the boundaries are hit within which the situation is to be studied, thus the analysis applies to the issues on the natural ground [55].

b. Solution Phase

Solving Equations: In that function, the system of linear or nonlinear algebraic equations, previously given during the preprocessing period, gets solved simultaneously. The balance between symbols (numbers of nodes) and tendencies (heat conduction behaviour) determines the outcome (values of displacements for different nodes) [55].

c. Postprocessing Phase

Result Analysis: The rendering stage is the takeoff point where the analysis goes into production. This is also where the crucial remaining information about mapping the core principle stresses and having valid data points of the hot spots are considered. Knowing this

fact is very important in unravelling the study's outcomes, selecting the designs, determining the improvements that can be made, and determining where further research should aim [55].

3.4.3 Finite element Application

- a. **Thermal and Fluid Flows:** FEM plays a crucial role in the solution of partial differential equations of heat and fluid flow-related problems, including modulating phenomena such as shock flows and acoustic transmission. This also involves the use of FEM in solving the Burger's Equation, a fundamental equation in thermal and fluid flow analysis [56].
- b. **Biomedical Applications:** The human body and its parts have complex geometry. As such, FEM is a very useful tool for modelling biomedical problems and treatments. Such applications cover percutaneous valve implantation, tissue modelling and deformation of body parts. In dentistry, FEM is of particular use in cases of non-carious cervical lesions, root canal treatment, restoration of root-filled teeth, and the study of shrinkage of composite and resin cement [56].
- c. **Plate Dynamics:** FEM is applied for the analysis of the bending deformation in the plate structures in terms of natural frequencies and mode shapes. This impacts many engineering processes, such as predicting the sheet metal blanking process outcomes [56].
- d. **Industrial and Business Management:** FEM helps design and develop products, and forecasts manufacturing times, costs, and wastage levels. In applications, virtual resistance values are used for furniture and sports products, optimization and design of tennis rackets and ice hockey sticks, and musical instruments, where dynamic and vibration analyses are applied for sound quality [56].
- e. **Computer Animation for Visualization:** FEM brings a revolution into special effects in films and video games by producing realistic pictures. It helps visualise architectural details, vehicle deformation, and naturally occurring disaster simulations for improved understanding and planning [56].

3.4.4 ANSYS Software

ANSYS software is a leading solution for engineering simulation, providing unique possibilities for both single-physics and Multiphysics simulations. ANSYS solutions are

known for their advanced technologies and seamless integration with many computer-aided design (CAD) software, helping engineers easily accomplish their tasks [57].

Integration and Compatibility: ANSYS works harmoniously with most industrial CAD systems, such as Pro-Engineers, AutoCAD, and Solid Edge, acting as a strong base for engineering simulations [57].

Solver Technologies and Simulations: Powered by advanced solver technologies, ANSYS can solve complex simulations that include multi-physics, user-customizable meshing technologies for specific physics requirements, and full computational fluid dynamics [57].

Application Spectrum: ANSYS can be applied to structural, thermal, fluid mechanics, acoustics, and Multiphysics problems. This encompasses linear and nonlinear behavior analyses, dynamic and static conditions, heat transfer, fluid flows and acoustic effects [57].

Multiphysics Capability: The software is mainly known for its Multiphysics simulations, including thermal-mechanical, thermal-electric, and other sophisticated interactions [57].

Software Family: ANSYS's versatility is not limited to a single program but to a family of specialized CAD programs, which makes it advantageous for specific simulation needs such as magnetic field analysis (ANSYS/Emag), fluid mechanics (ANSYS/Flotran), and dynamic simulations (ANSYS/LS-DYNA) [57].

3.5 COMPOSITE MATERIAL

3.5.1 Introduction

Composites are hybrid materials that are made by mixing at least two elements. Through such assortment, a new class of material science is created. Achieved through the combination of fibre or particles, these organic material matrices form one material, as a whole, in the presence of polymers, metal or ceramic. This an apparent, bring out the desired and mere traits that none of the materials could bring individually. The advancement of the composition, which began with larger intrinsic parts and has progressed to the use of carbon nanotubes and nanofibers with nanotechnology, touches all the sectors and strongly confirms its importance. Being naturally present for a long time of human civilization and invention, composites have turned out to be one of the most efficient materials in present-day engineering and technology. Blending epoxy with fibres shortens the required length while stiffness and elasticity are enhanced. Such 3D printing technologies not only enable

applications that require a combination of high strength, stiffness, low thermal expansion, simultaneous thermal insulation, energy harvesting and self-repair but also contribute to other areas that may require them. Regional materials' growth is a perfect example of human creative thinking, and it proves that we search for the most effective ways to use the offered materials and to design them [58].

3.5.2 Classifications of Composite Materials

a. Powder Metallurgy (P/M) techniques, used for producing Metal Matrix Composites (MMCs), are one of the most promising manufacturing processes for MMCs [59].

Metal matrix composites are metal matrices with a reinforcement material, which may be ceramic or metallic fibers. Thus, such composites are associated with better base metal properties, like high strength, stiffness, or resistance to wear and corrosion. Manufacturing Techniques: Methods comprise of high-pressure infiltration, mould compression molding, infiltration vacuum mold, and pressure less metal intrusion. MMCs find applications in industries where materials need to bear high temperature and highly corrosive environment. The applications can be found in aerospace, automotive, and electronics, where materials like carbon graphite/copper, graphite/aluminum, SiC/aluminum, and SiC/magnesium are used [59].

b. Polymer Matrix Composites (PMCs)

PMCs are composed of resin polymer matrix and are reinforced with fibers such as glass, carbon, or aramid. Their properties are light weight, high strength, and corrosion resistance. Thermosets are a type of resin (e.g., epoxy, polyester) known for their stiffness and strength when cured. Thermoplastics (e.g., polypropylene, nylon) that can be reshaped and reused. PMCs are popular in the automotive, aerospace, marine, and construction industries because they are used to produce parts that have a high strength-to-weight ratio. They provide design freedom and are used to produce vehicle bodywork panels, structural elements in aircraft and boats [59].

c. Composed of Ceramic fibres (CMCs.)

CMCs are composed of ceramic fibres in a ceramic matrix. They have a high melting point and good thermal stability, and are wear- and corrosion-resistant, therefore ideally suited for high-temperature applications. Excellent mechanical strength, good flexibility, and high

service temperature exceeding 1500°C. As a result of the fact, they can function under harsh conditions, CMCs are applied in aerospace for components such as turbine blades, in automotive for brake systems, and in the energy sector for heat exchanger tubes [59].

3.5.3 Using Composite Materials in Aerospace Applications

Manufacturing composite materials has materially improved in the aerospace sector thanks to its creative mix of strength and ultimate stability coupled with low-weight impact. Among them, framework and fibre composite materials such as Carbon fibre-reinforced composites (CFRC) and glass-reinforced plastic (GRP) are manufactured to fit aerospace demands and play a role in aircraft's general performance and efficiency. Typically, a composite material involving various layouts of its primary parts is used in several areas, including the construction of components or electric insulation. It is indeed the adaptability of these composites as well as their resistance to unfavorable factors such as problematic ones such as structural fatigue and wears that make these composites much needed in modern aerospace, in which weight reduction should not come down to sacrificing strength, durability, and corrosion resistance [60].

On the other hand, the composite materials' hazardous qualities and potential threats for safety in aerospace require in-depth studies. Problems analogous to delamination which happens when the laminate layers are separated and the possibility of fiber detachment from the matrix, proves that carefully designed and developed technologies by the manufacturers is necessary. The special machines like autoclaves for processing composites as a determinant of manufacturing technology investment in the aerospace industry, where the industry relies on such machines. Moreover, by changing from such regular materials such as titanium alloys and aluminum to the composites, we stumble upon many difficulties like mechanical strength and fuel consumption, but also the new challenges related with static, fatigue and stress load managing. These issues underscore the sophisticated nature of composites in aerospace projects, requiring more efforts from the engineers to make these innovations a reality, along the line, mitigate their disadvantages [60].

3.5.4 Failure Criteria

3.5.4.1 Maximum stress criterion

The Maximum Stress Criterion for orthotropic laminae is an extension of the maximum standard stress theory that applies to the isotropic materials. This criterion fails in case any of the principal stress components along the material axis exceeds its corresponding strength. For the Maximum Stress Criterion, ensuring a composite material does not fail according to this criterion, are expressed as [58] :

For longitudinal stress (σ_1) (along the fiber direction):

$$-sL(-) < \sigma_1 < sL(+) \quad (3.7)$$

For transverse stress (σ_2) (perpendicular to the fiber direction):

$$-sT(-) < \sigma_2 < sT(+) \quad (3.8)$$

For shear stress τ_{12} (in the plane of the lamina):

$$|\tau_{12}| < sLT \quad (3.9)$$

where $sL(+)$ and $-sL(-)$ are the tensile and compressive strengths in the longitudinal direction, respectively. $sT(+)$ and $-sT(-)$ are the tensile and compressive strengths in the transverse direction, respectively, and sLT is the shear strength.

3.5.4.2 Maximum strain criterion

The Maximum Strain Criterion, introduced in 1967, is used to forecast the failure of orthotropic laminae so that it is considered as an extension of the maximum normal strain theory for isotropic materials. This factor states that failure happens when any principal material axis strain component exceeds the corresponding ultimate strain. To avoid failure under this criterion, the material must satisfy the following inequalities [58]:

The longitudinal strain ϵ_1 must remain within the bounds of the ultimate compressive strain $-eL(-)$ and the ultimate tensile strain $eL(+)$. The transverse strain ϵ_2 must stay within the limits set by the ultimate compressive strain $-eT(-)$ and the ultimate tensile strain $eT(+)$. The absolute value of the shear strain γ_{12} must not exceed the ultimate shear strain e_s [58].

$$-eL(-) < \epsilon_1 < eL(+) \quad (3.10)$$

$$-eT(-) < \varepsilon_2 < eT(+) \quad (3.11)$$

$$|\gamma_{12}| < eLT \quad (3.12)$$

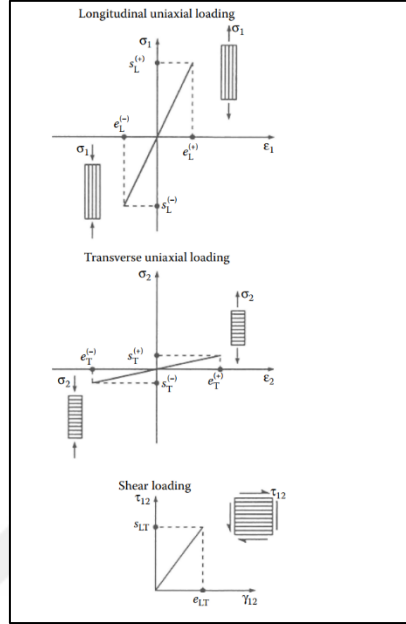


Figure 3.6: Shows the Stress-Strain Relationships Under Uniaxial and Shear Loading Conditions, Highlighting the in-Plane Strengths and Ultimate Strain Limits of a Lamina [58].

3.5.4.3 Tsai-Wu failure criterion

The Tsai-Wu failure criterion provides a universal way of failure prediction of anisotropic materials, such as composites, by considering the intricate interrelations of various stress components. This criterion is particularly convenient for engineering of composite materials because materials tend to have strength in different directions because of their anisotropic character [58].

$$F_i \sigma_i + F_{ij} \sigma_i \sigma_j = 1 \quad (3.13)$$

In this equation, $i, j = 1, 2, \dots, 6$ correspond to the stress components in a contracted notation, and F_i and F_{ij} are material-specific constants determined through experimentation. This criterion considers both the individual stress components and their interactions. To predict failure accurately, the criterion stipulates that the equation's left side must not exceed 1, with failure predicted when this value reaches or surpasses 1.

3.5.4.4 Tsai-hill failure criterion

The Tsai-Hill criterion reduces the Tsai-Wu criterion under certain assumptions regarding equal tensile and compressive strengths for predicting failure in composite materials. This criterion is based on the von Mises yield criterion and is modified to consider the anisotropy in composite materials [58]. For cases of plane stress, where $\sigma_3, \sigma_{33}, \sigma_{34}, \sigma_{35} = 0$ the Tsai-Wu criterion simplifies to [58]:

$$F_{11}\sigma_1^2 + F_{22}\sigma_2^2 + F_{66}\tau_{12}^2 + F_1\sigma_1 + F_2\sigma_2 + 2F_{12}\sigma_1\sigma_2 = 1 \quad (3.14)$$

Here, $F_{11}, F_{22}, F_{66}, F_1, F_2,$ and F_{12} are the material constants for the composite, σ_1 and σ_2 are the normal stresses, and τ_{12} is the shear stress in the plane of the lamina.

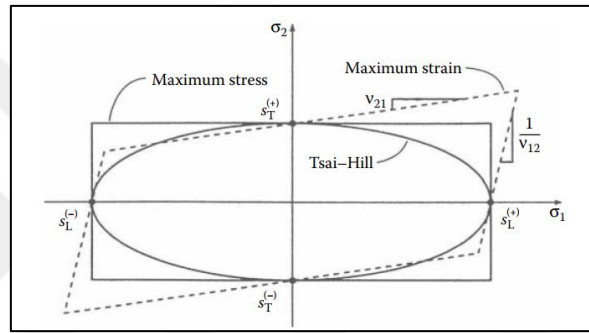


Figure 3.7: Shows the Failure Surfaces for the Maximum Stress, Maximum Strain, and Tsai-Hill Criteria in σ_1, σ_2 Stress Space, Demonstrating How Each Criterion Predicts the Material Failure Under Different Stress Conditions [58].

3.5.4.5 Inverse reverse factor and safety factor

a. Safety factor

Safety factor is an essential principle of engineering designing aimed at providing that a system or component works under the given conditions without failing. It is the relation between the capacity that is the strength, and the demand which can be referred to as load or stress that is applied to the system. This ratio characterizes the built-in safety margin in a design to cater for the uncertainties in the load and strength, material property variation, manufacturing tolerances, and unexpected operational stresses. The safety factor is used to guarantee that even if the estimated load will increase or the material strength will decrease because of variations or unforeseen conditions, the system will continue to perform its required function without failure. It is a safety measure to reduce the failure hazard by making the structures and components oversized that provides them with a margin of

safety to withstand surprise loads or weaknesses [61]. Safety factor could be calculated by the following equation [61]:

$$n = \frac{S}{\sigma} \quad (3.15)$$

where S is the material strength (or ultimate strength) and σ is the allowable stress.

i. If the $n > 1$ The composite is safe.

ii. If the $n < 1$ The composite fails.

b. Inverse reverse factor

The Inverse Reverse Factor (IRF) is proposed as a critical parameter to evaluate the failure susceptibility of the composite materials. IRF is employed to forecast composite failure, that is the load value/ IRF. There are two cases for it [62]:

i. $IRF > 1$: The composite fails. This indicates that the load applied to the composite exceeds its capacity to withstand that load, leading to failure.

ii. $IRF < 1$: The composite is safe. This means the composite can safely endure the load without failing.

3.6 NATURAL FREQUENCY

3.6.1 Introduction

Natural frequency analysis is a technique that is utilized to identify the frequencies at which drives vibrate or structural components self-oscillate due to an intrinsic vibration under conditions of a disturbance [63]. In the case of UAV (Unmanned Aerial Vehicle) fixed wings, numerical analysis is of the essence in ascertaining frequencies that just might resonate with operational/environmental vibrations input. For instance, resulting vibrations may cause structural weakness to the point that the UAV can't perform well or even be deemed safe due to this. Keeping the UAV's fixed wings deal with the vibrations they generates outside the resonant frequencies is the most critical way to avoid aerodynamic phenomena that may lead to flutter, which is an oscillation that quickly becomes uncontrollable, unless it is stopped, it will continue to auto destruct through these uncontrollable oscillations [63].

3.6.2 Natural Frequency Formulas

a. General Formula for Natural Frequency [63].

$$f = \frac{1}{2\pi} \sqrt{\frac{EI}{\mu}} \quad (3.16)$$

The natural frequency (f) of a wing of a UAV can be obtained through this equation, where E denotes the Young's modulus of the material (stiffness), I stand for the second moment of inertia of the cross-section of the wing (bending resistance), and μ is the mass per unit length of the wing. This equation emphasizes that the vibrational properties of a wing are closely connected with its materials properties and mass distribution [63].

b. Mass per Unit Length (μ)

$$\mu = \rho A + \mu_{\text{additional}} \quad (3.17)$$

This equation determines the wing mass per unit length of a UAV. ρ wing the density of the wing material, Area A is, and $\mu_{\text{additional}}$ considers any excess weight from the components or the payloads which are embedded within the wing. This equation makes sure that the inherent weight of the wing and the added weight from equipment or payload are considered in the analysis [63].

3.7 AAI SHADOW -200 RQ-7 UAV DESIGN AND NUMERICAL ANALYSIS

The AAI RQ-7 Shadow UAV is a high lift, low speed air vehicle developed by the US Army. This type of UAV is designed for missions that need a higher load capacity, reduced take-off and landing distances, and low stall speed. It is but an element of a wider trend in UAV research aimed at increasing operational effectiveness in different types of missions, such as, rescue operations, spying, and even firefighting. The evolution of RQ-7 Shadow in this context is in fact a substantial tendency to use UAVs beyond the traditional military purposes, as some private businesses also participate in developing UAVs for various civilian and humanitarian activities. As such, the aerodynamic design process of these UAVs requires choosing high lift and low Reynolds number aerofoils, emphasizing the need for performance analysis and comparison of these aerofoils. As a result, this UAV type represented by the RQ-7 Shadow has been of much interest in aerospace engineering, especially in the research and development of aerofoils that would satisfy the specific requirements of low speed, high lift UAV operations [64].



Figure 3.8: AAI Shadow -200 RQ-7 UAV [65].

3.7.1 AAI Shadow -200 RQ-7 UAV Design

The software used in this research for the UAV model design is SOLIDWORKS. The design of the UAV will be like the actual form and sizes available on the market, with slight changes. These changes will provide an opportunity for the aspect of new dimensions, including the analysis of composite materials, to be trialed since this is the main subject of this research.

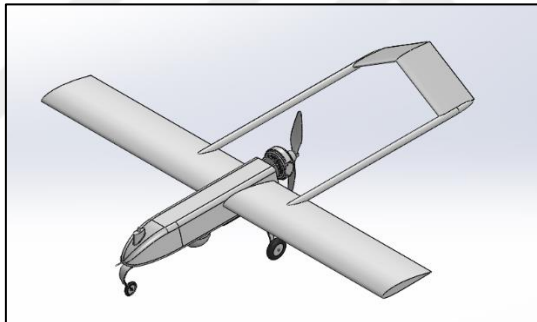


Figure 3.9: AAI Shadow -200 RQ-7 UAV Model.

The table below shows all dimensions of the UAV.

Table 3.1: Dimensions of RQ-7 UAV.

Parameter	Value
Length	3.98 m
Height	2 m
Wingspan	4.43 m

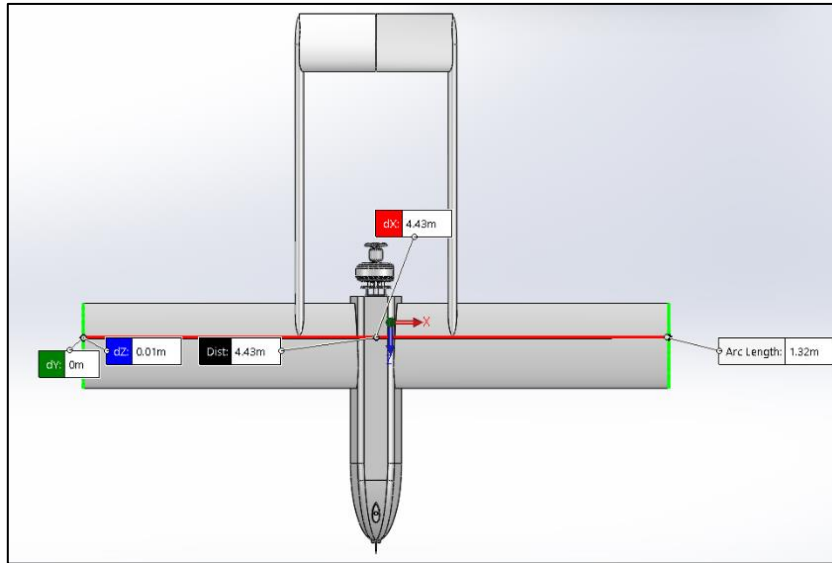


Figure 3.10: Dimensions of Wingspan.

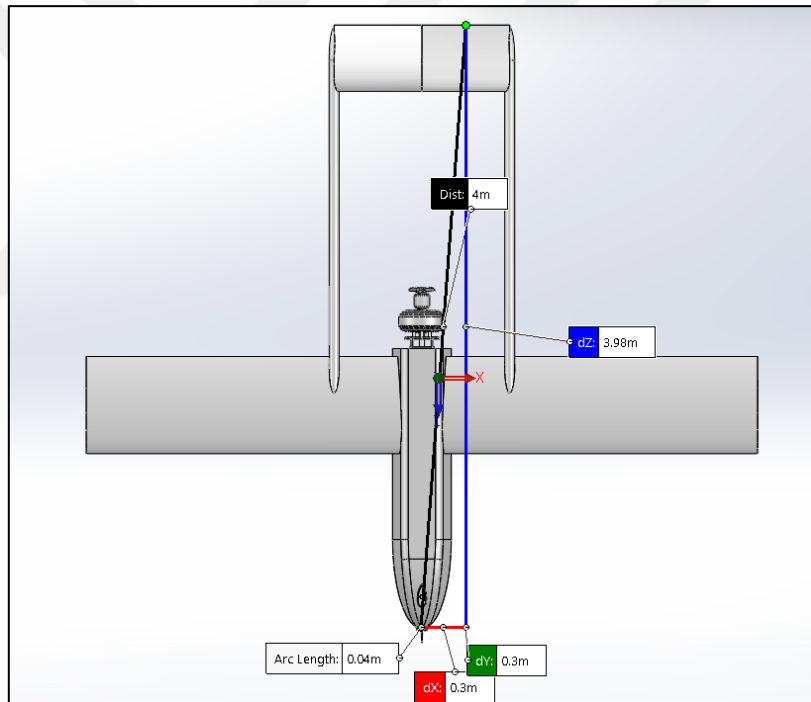


Figure 3.11: Dimensions of Total Length.

However, the study will be conducted on the UAV's wing because it is the most appropriate part to place composite materials on.

Therefore, the wing was separated from the plane, as the picture below shows.



Figure 3.12: AAI Shadow -200 RQ-7 Wing Length.

ANSYS software studies the CFD on a UAV, but before that, the UAV is placed in the fluid domain designed by SOLIDWORKS to form a tunnel for the air to be studied in the next section, which is what the figures below show.

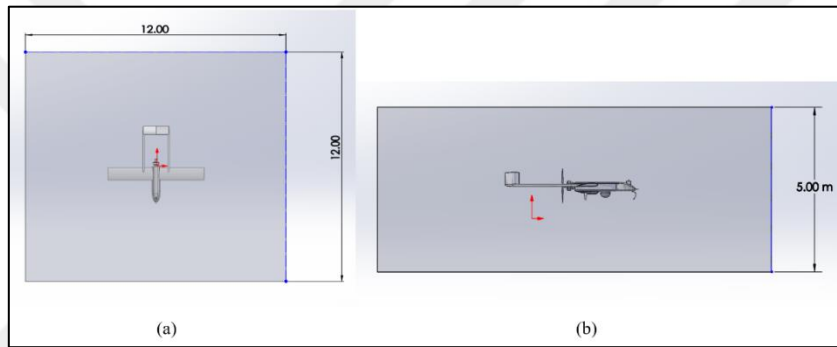


Figure 3.13: RQ 7 UAV in Fluid Domain.

However, as explained, the focus of the study will be on the wing, so it has been placed as a unit in the fluid domain, as in the figure below.

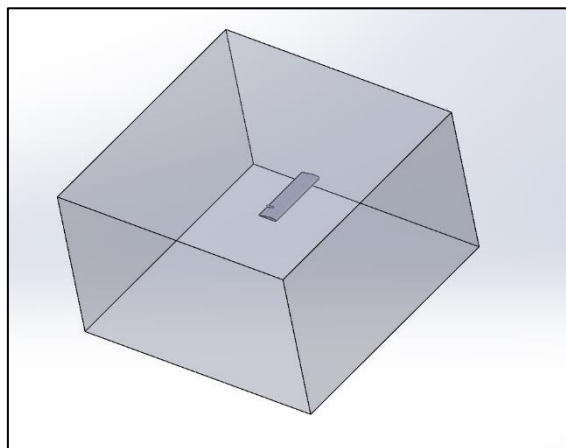


Figure 3.14: RQ 7 UAV Wing in the Fluid Domain.

Table 3.2: Properties of the Fluid Domain.

Parameter	Value
Total Domain Length	12 m
Total Domain Width	12 m
Total Domain Hight	5 m

3.7.2 AAI Shadow -200 RQ-7 UAV Numerical Analysis

This section will be dedicated to detailed numerical research on the topic, which will be divided into several subsections. At the start, Computational Fluid Dynamics (CFD) analysis will be conducted on an aircraft wing at its maximum speed to determine the forces and pressures acting on the wing. Then, the first case study of this thesis will be performed, where the analysis of Fluid-Structure Interaction (FSI) will be conducted. The results from the CFD analysis will be combined here with a static structural analysis, to explore what affect the forces have on the aluminium structure of the aircraft.

After the FSI analysis, a modal analysis will be performed to find the natural frequencies and mode shapes of the structure. This study will give more information about different vibration modes and frequencies that are related to them.

In the second and third case studies, the same wing will be considered; however, composite materials will be included. The composite material for the second case will be Composite, Epoxy/glass fiber, UD prepreg, QI, while for the third case, the material will be Epoxy Carbon UD (230 GPa) Prepreg. These materials will be defined, and layup configurations specified with the help of the ACP (ANSYS Composite PrepPost) module.

Once the composite materials and their layups are specified, the wing will be connected back to the static structural analysis to complete the FSI and modal analyses, like the first case. The first case study aims to verify the structural strength of the aircraft under the specified conditions. However, the main comparison will be between the second and third cases to identify the best-performing composite material.

This numerical study will provide helpful information about the behavior of the aircraft wing in different situations, as well as the advantages of using various composite materials.

Results obtained from these analyses will give an overall picture of the structural response of the wing and will allow rational judgments on its layout optimization.

3.7.2.1 CFD analysis

a. Mesh analysis

The first step is to create a mesh for the fluid domain around the UAV wing to get precise results in CFD analysis. Mesh settings and quality metrics are important for achieving an accurate and reproducible outcome. The figures and table that follow indicate the mesh generation process and its settings.

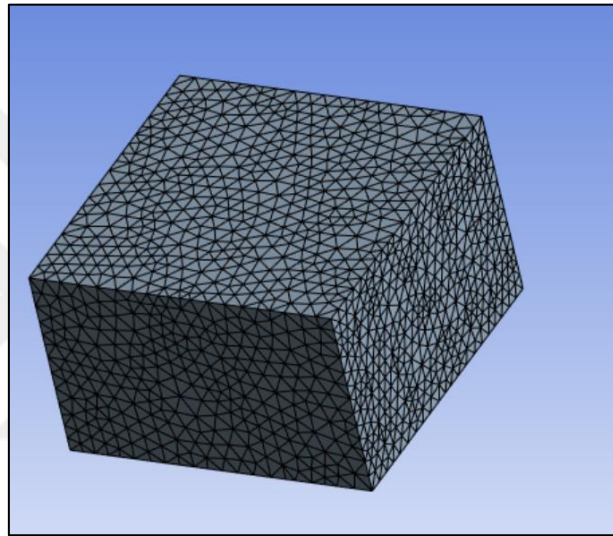


Figure 3.15: Mesh Results on Whole Fluid Domain.

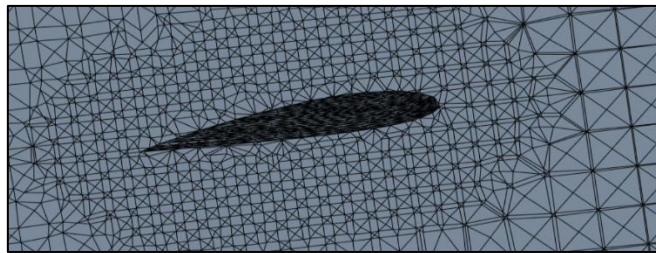


Figure 3.16: Mesh Results on Whole Fluid Domain.

The mesh settings used are in the table below.

Table 3.3: Mesh Settings for Fluid Domain.

Mesh Method	Tetrahedrons
Algorithm	Patch independent
Max Element Size	400 mm
Min Element Size	70 mm
Face sizing	50 mm

The boundary conditions for the CFD analysis were appropriately defined to represent the fluid domain and flow conditions accurately. The inlet of the fluid domain was specified as a velocity-inlet, the outlet as a pressure-outlet, and the wing body and remaining surfaces as wall boundaries. These boundary conditions ensure that the flow physics is correctly captured in the computational domain, allowing for reliable and physically meaningful results from the CFD simulations.

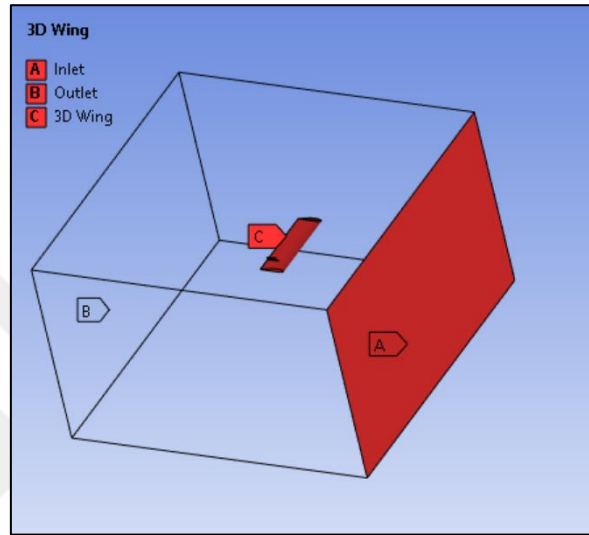


Figure 3.17: Boundary Conditions of Fluid Domain for RQ-7.

b. Ansys Fluent Setup

After completing the mesh, the analysis settings were defined in Setup and presented in the table below.

Table 3.4: ANSYS Fluent Analysis Setup Settings.

Iterations:	1000
Scheme	coupled
Gradient	Least Squares Cells Based
Pressure	Second Order
Viscous Mode	k-epsilon (eqn) Realizable

As discussed in the introduction of this section, the study was conducted at the UAV's maximum speed to ensure a more accurate structural analysis. According to previous research, the RQ-7 UAV's maximum speed is 218 km/h [66].

3.7.2.2 FSI analysis

As previously explained, there are two types of FSI: unidirectional and bidirectional. In contrast, one-way FSI is more desirable for aircraft wings as the concern here is upon the effect of aerodynamic forces upon the aircraft structure rather than the influence of the structure upon the airflow. In one-way FSI, the fluid forces are communicated to the structure, but the structural deformations are not relayed to the fluid domain. This is a frequently used approach in the analysis of aircraft wings, as the main concern is the influence of the airflow on the structural behavior. Therefore, one-way FSI was utilized in this study to examine the interrelation of the aerodynamic forces and wing structure.

Therefore, this analysis will require a 3D solid aluminium wing. As previously mentioned, the first step will be generating a wing mesh.

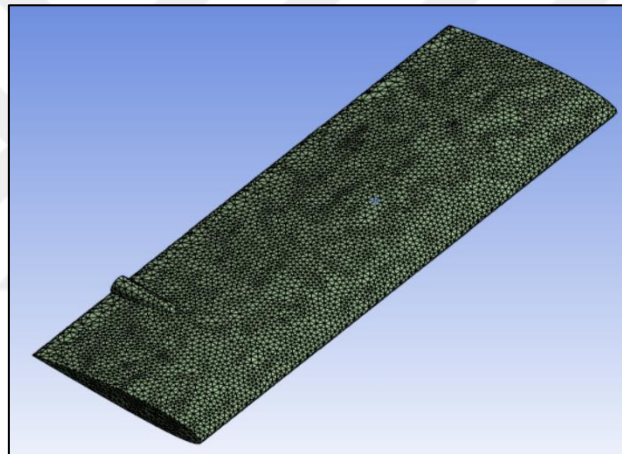


Figure 3.18: Mesh Results on 3D Wing of RQ-7 UAV.

In this analysis, the fixed support is applied at the end of the wing attached to the UAV. The load is the Imported Pressure obtained from the ANSYS Fluent results, as shown in the figure below.

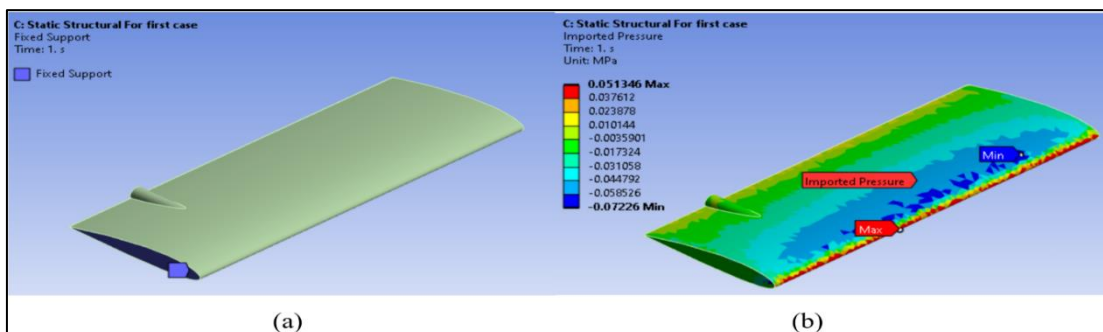


Figure 3.19: (a) Shows the Fixed Support and (b) The Imported Pressure Load on the RQ-7 UAV.

The stress and strain values, safety factors, and other relevant parameters will be presented and discussed in the next chapter.

3.7.2.3 ACP composite materials analysis

The ACP (ANSYS Composite PrepPost) module will be utilized for the second and third case studies involving composite materials on the UAV's wing. This module allows for the specification of composite material types, thicknesses, and layup configurations to represent the composite structure accurately in numerical analysis.

As mentioned previously, the two composite materials that will be used in this study are Composite, Epoxy Carbon UD (230 GPa) Prepreg, and Composite, Epoxy/glass fiber, UD prepreg, QI. Their properties are listed in the tables below.

Table 3.5: Composite, Epoxy Carbon UD (230 GPa) Prepreg [67].

Density (kg/m ³)	Young's Modulus (GPa)	Poisson's Ratio	Shear Strength (MPa)	Shear Modulus (GPa)	Tensile Strength (MPa)
1490	121	0.4	60	4.7	2231

Table 3.6: Composite, Epoxy/Glass Fiber, UD Prepreg, QI [68].

Density (kg/m ³)	Young's Modulus (GPa)	Poisson's Ratio	Shear Strength (MPa)	Shear Modulus (GPa)	Tensile Strength (MPa)
1840	21	0.31	33	9.23	504

Ten layers of composite material, each 0.5 mm thick, will be added to each composite material case, resulting in a total thickness of 5 mm on the aircraft wing.

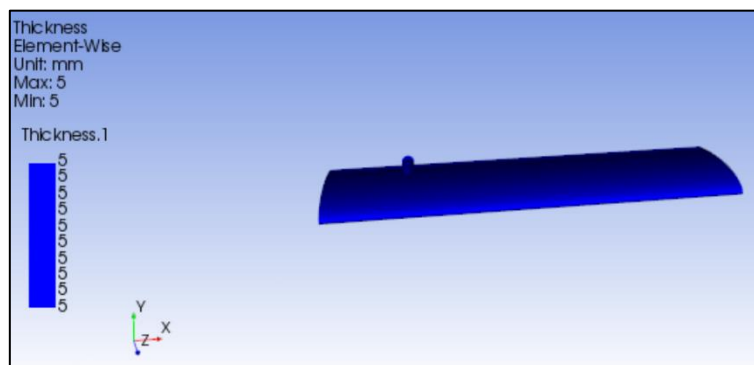


Figure 3.20: RQ-7 Wing after Composite Material Added.

After placing the composite material, the wing was re-linked in the Static Structure window to transfer the properties of the composite material to the FSI analysis and obtain the results.

3.7.2.4 Modal analysis

In this analysis, the Modal Analysis, the natural frequencies of the UAV's wing will be studied using the Modal Analysis module provided by ANSYS. The Modal Analysis will be coupled with the results obtained from the FSI analysis, specifically from the Static Structural module, to determine the natural frequencies.

The figure below shows the project schematic for the first case study involving the aluminium wing without composite materials.

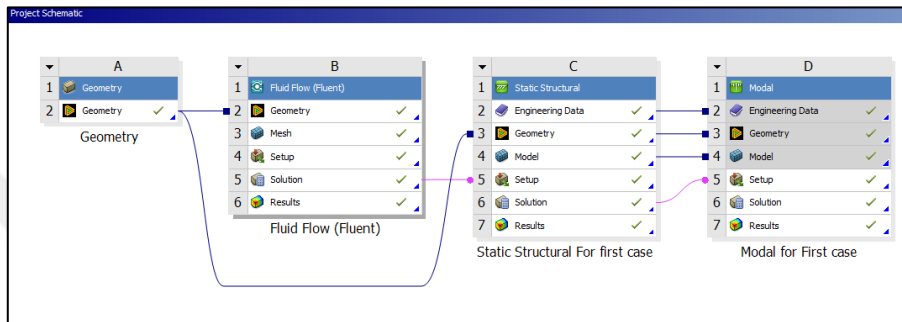


Figure 3.21: Project Schematic for the First Case Study.

For the second and third cases involving the use of composite materials, the project schematic is as shown in the figure below.

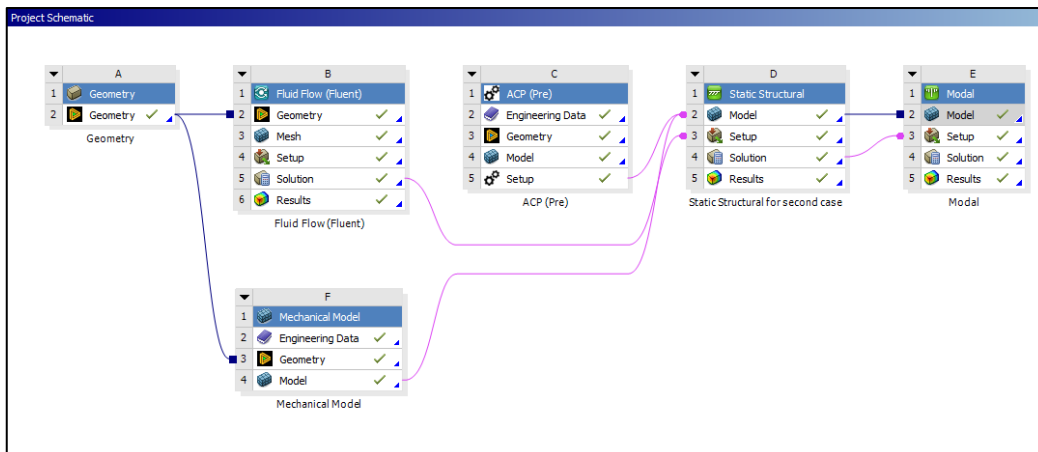


Figure 3.22: Project Schematic for the Second and Third Case Study.

4. RESULTS AND DISCUSSION

In this chapter, the main results from the numerical analyses will be presented and discussed in detail. First, the findings from the Computational Fluid Dynamics (CFD) simulations, which provide information about the forces and pressure acting on the aircraft wing, will be explained. After that, the three case studies involving the fluid-structure interaction analyses and modal analyses will be explored.

The first case serves as a baseline, validating the structural adequacy and vibrational characteristics of the aluminium wing under the defined aerodynamic loading conditions. Nonetheless, the attention will be paid to the comparison of the second and third case studies that deal with the use of different composite materials for the wing structure. This evaluation will be done by comparing the results of these two cases in order to judge the benefits and performance enhancements offered by each composite material configuration.

As a result of this comprehensive investigation, much useful information will be gained concerning the behaviour of the wing structure, its vibrational features, and its possible ways of failure in the impact of applied aerodynamic loads. This chapter aims to identify the most appropriate composite material solution that yields superior structural performance, better vibrational characteristics, and increased safety margins for the wing of the aircraft under study.

4.1 CFD ANALYSIS RESULTS

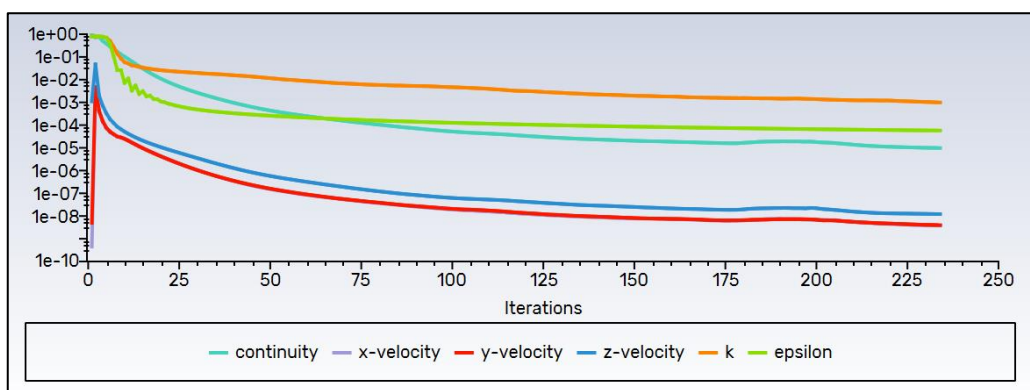


Figure 4.1: Convergence of Solution of CFD Analysis.

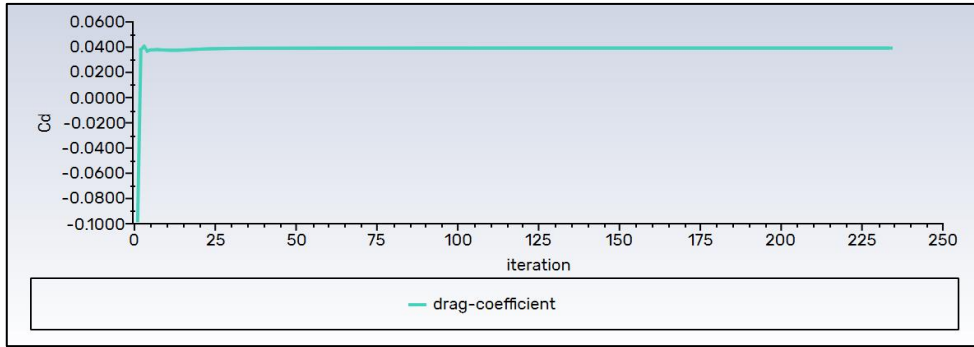


Figure 4.2: Value of Drag Coefficient Against Solution Iterations.

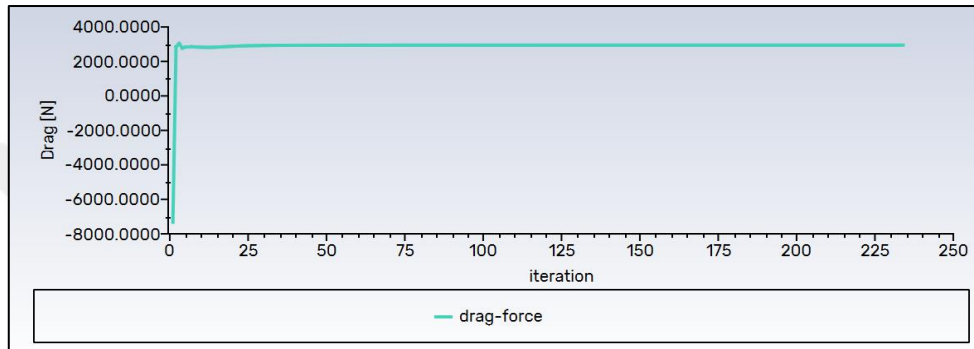


Figure 4.3: Value of Drag Force Against Solution Iterations.

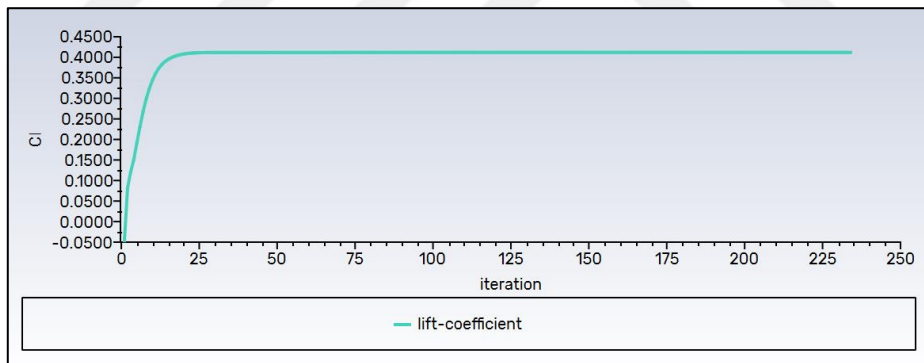


Figure 4.4: Value of Lift Coefficient Against Solution Iterations.

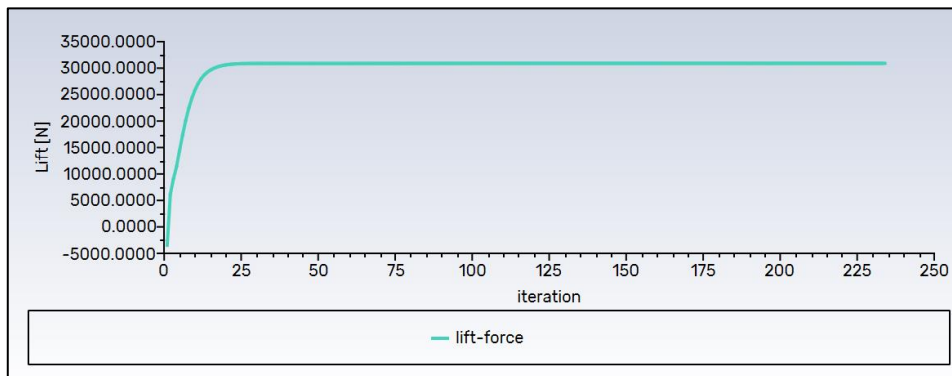


Figure 4.5: Value of Lift Force Against Solution Iterations.

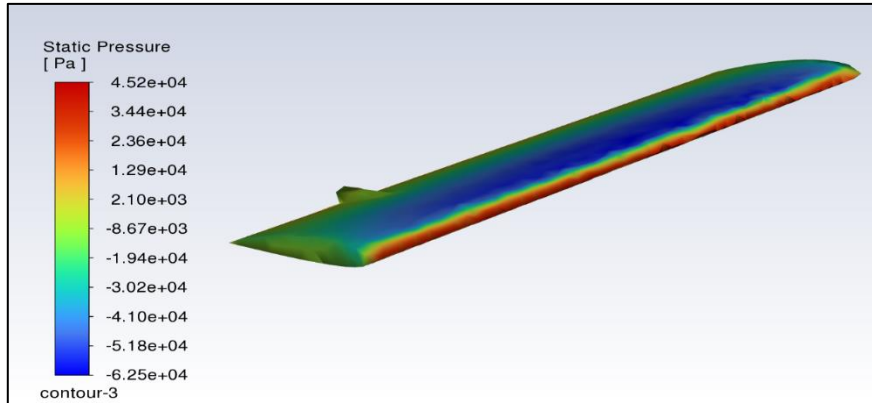


Figure 4.6: Shows the Pressure Contours on the 3D Wing.

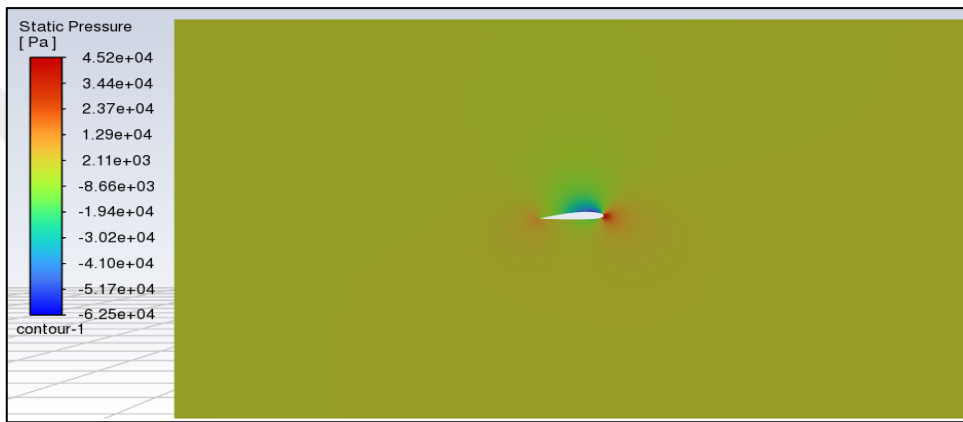


Figure 4.7: Shows the Pressure Contours on the 2D Section of Wing.

Table 4.1: Results of CFD Analysis

Parameter	Value
Drag coefficient	0.04
Drag force	2944(N)
Lift coefficient	0.41
Lift force	30905.83 (N)
Iterations for convergence	241

4.2 FIRST CASE STUDY RESULTS

4.2.1 FSI Analysis Results

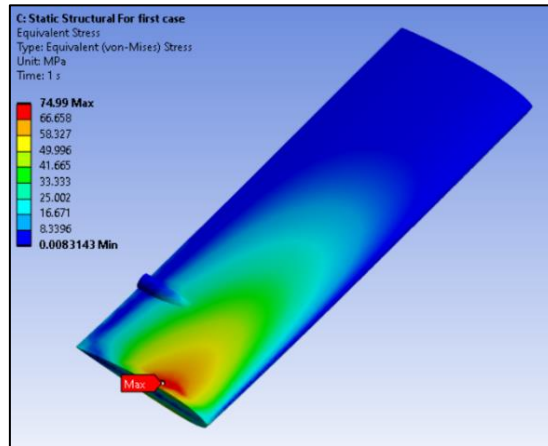


Figure 4.8: Maximum Von-Mises Stress on RQ-7 Wing When the Material is Aluminium.

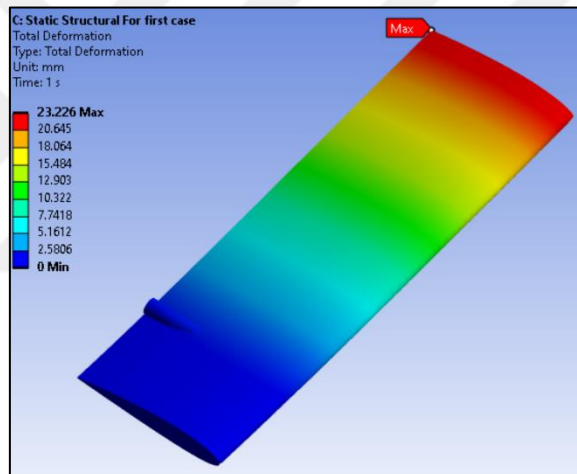


Figure 4.9: Total Deformation on RQ-7 Wing When the Material is Aluminium.

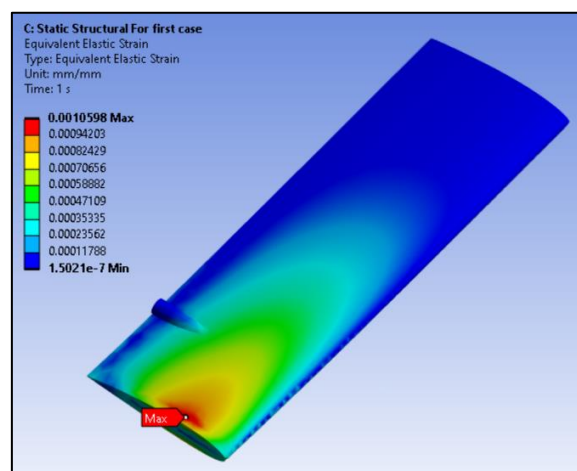


Figure 4.10: Equivalent Elastic Strain on RQ-7 Wing When the Material is Aluminium.

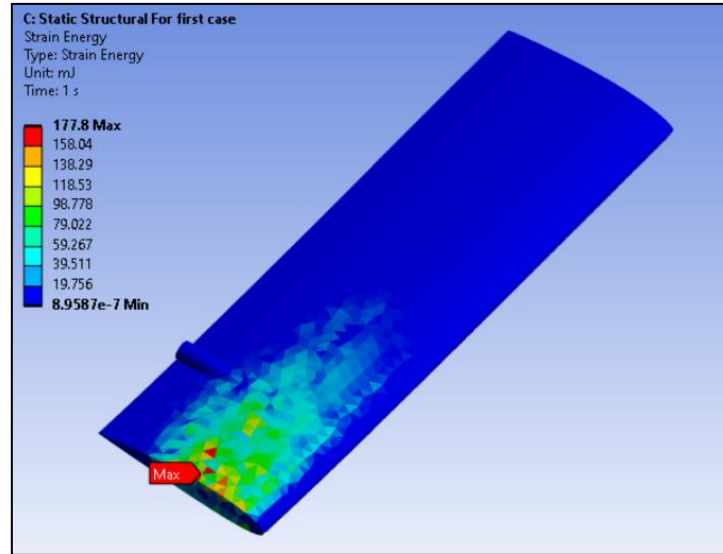


Figure 4.11: Strain Energy of RQ-7 Wing When the Material is Aluminium.

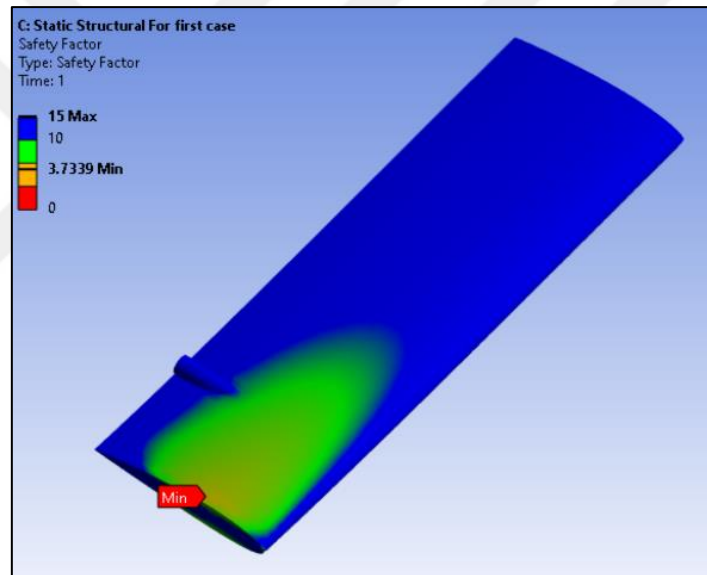


Figure 4.12: Safety Factor of RQ-7 Wing When the Material is Aluminium.

Table 4.2: Results of FSI Analysis for First Case.

Parameter	Value
Maximum Von-mises stress	74.99 (MPa)
Total Deformation	23.226 (MPa)
Elastic strain	0.00105
Strain Energy	177.8 (mJ)
Factor of safety	3.733

4.2.2 Modal Analysis Results

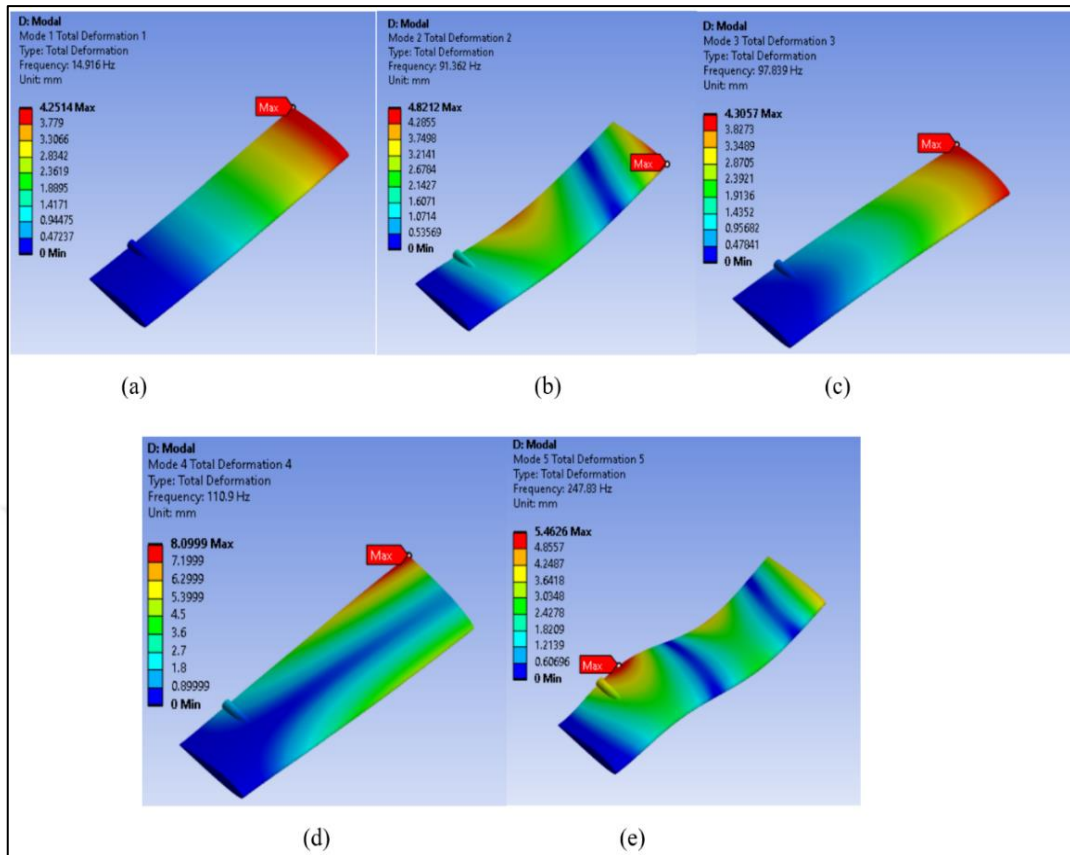


Figure 4.13: Modal Analysis Results of RQ-7 Wing When the Material is Aluminium: (a) Mode 1, (b) Mode 2 , (c) Mode 3, (d) Mode 4, (e) Mode 5 .

Table 4.3: Natural Frequencies of First Case Study.

Mode	Frequency [Hz]	Total Deformation (mm)
1	14.916	4.25
2	91.362	4.82
3	97.839	4.30
4	110.9	8.09
5	247.83	5.46

4.3 SECOND CASE STUDY RESULTS

4.3.1 FSI Analysis Results

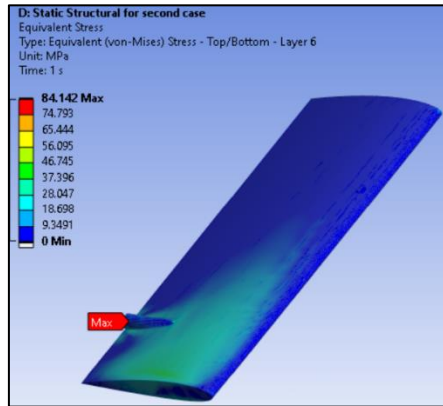


Figure 4.14: Maximum Von-Mises Stress on RQ-7 Wing When the Material is Composite, Epoxy Carbon UD (230 GPa) Prepreg.

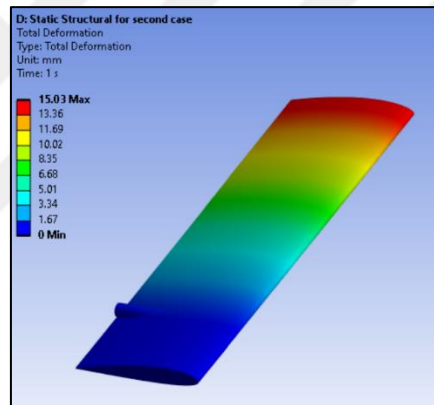


Figure 4.15: Total Deformation on RQ-7 Wing When the Material is Composite, Epoxy Carbon UD (230 GPa) Prepreg.

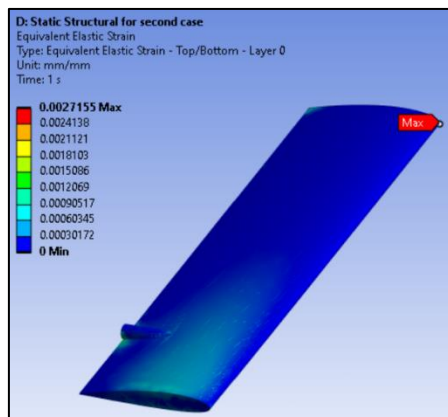


Figure 4.16: Equivalent Elastic Strain on RQ-7 Wing When the Material is Composite, Epoxy Carbon UD (230 GPa) Prepreg.

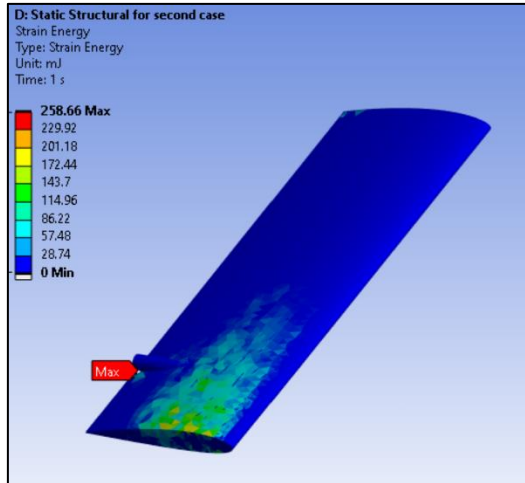


Figure 4.17: Strain Energy of RQ-7 Wing When the Material is Composite, Epoxy Carbon UD (230 GPa) Prepreg.

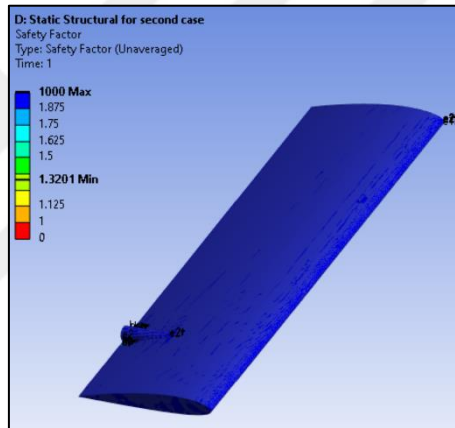


Figure 4.18: Safety Factor of RQ-7 Wing When the Material is Composite, Epoxy Carbon UD (230 GPa) Prepreg.

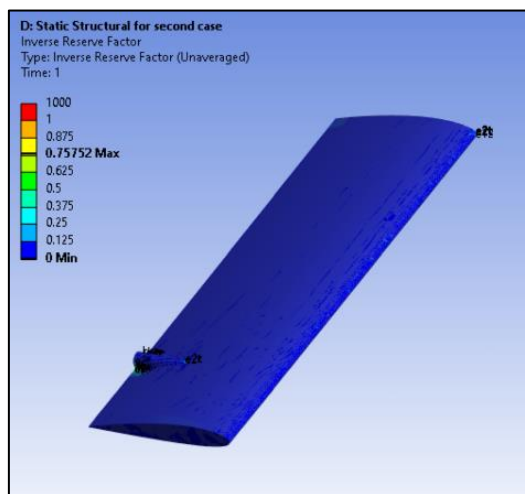


Figure 4.19: Inverse Reserve Factor of RQ-7 Wing When the Material is Composite, Epoxy Carbon UD (230 GPa) Prepreg.

Table 4.4: Results of FSI Analysis for Second Case.

Parameter	Value
Maximum Von-mises stress	84.142 (MPa)
Total Deformation	15.03 (MPa)
Elastic strain	0.00271
Strain Energy	258.66 (mJ)
Factor of safety	1.32
Inverse Reserve Factor	0.75

As was discussed earlier, the factor of safety must be more than 1 and the factor of inverse reverse must be less than 1 for the component to be considered safe. The design values with the smallest safety factor and the largest reverse inverse factor are chosen as the optimal design values. This technique is referred to as the optimum design method. In this study, the Maximum Strain criterion has been found to meet these requirements.

Table 4.5: Safety Factors Values for Different Criteria's for Second Case.

Criteria	Maximum Stress	Maximum Strain	Tsai-Wu	Tsai-Hill
Safety Factor (SF)	1.647	1.32	1.463	1.537

Table 4.6: Inverse Reserve Factor Values for Different Criteria's for Second Case.

Criteria	Maximum Stress	Maximum Strain	Tsai-Wu	Tsai-Hill
Inverse Reserve Factor (IRF)	0.637	0.757	0.682	0.644

4.3.2 Modal Analysis Results

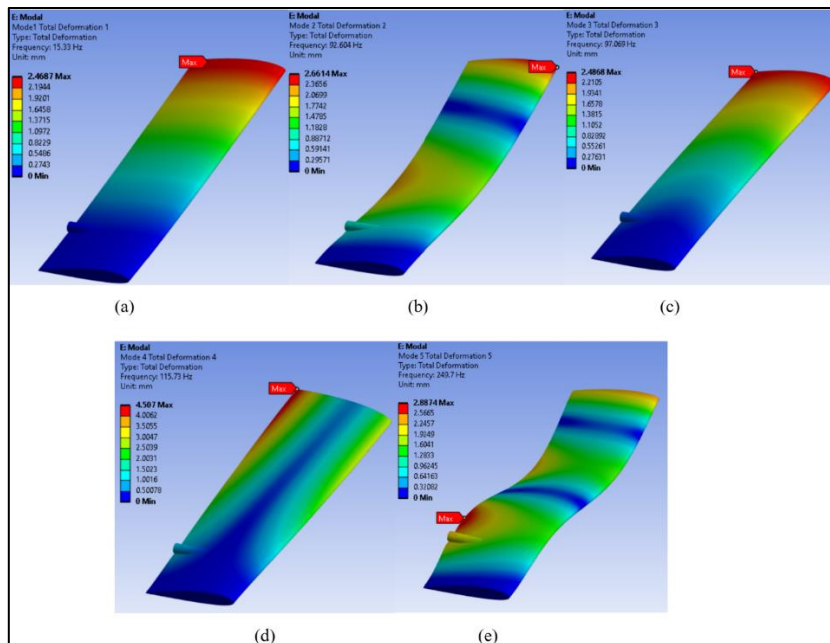


Figure 4.20: Modal Analysis Results of RQ-7 Wing when the Material is Composite, Epoxy Carbon UD (230 GPa) Prepreg.: (a) Mode 1, (b) Mode 2, (c) Mode 3, (d) Mode 4, (e) Mode 5.

Table 4.7: Natural Frequencies of Second Case Study.

Mode	Frequency [Hz]	Total Deformation (mm)
1	15.33	2.46
2	92.604	2.66
3	97.069	2.48
4	115.73	4.50
5	249.7	2.88

4.4 THIRD CASE STUDY RESULTS

4.4.1 FSI Analysis Results

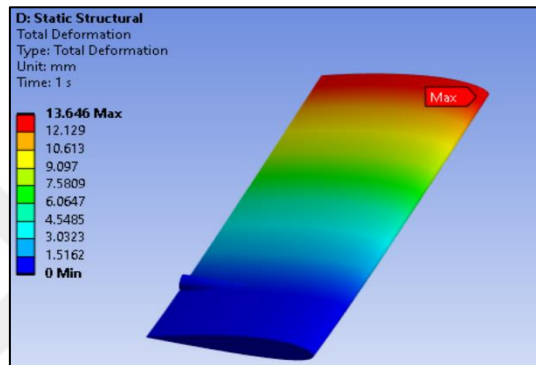


Figure 4.21: Total Deformation on RQ-7 Wing When the Material is Composite, Epoxy/Glass Fiber, UD Prepreg, QI.

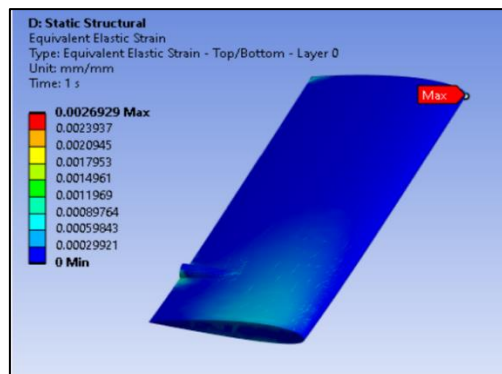


Figure 4.22: Equivalent Elastic Strain on RQ-7 Wing When the Material is Composite, Epoxy/Glass Fiber, UD Prepreg, QI.

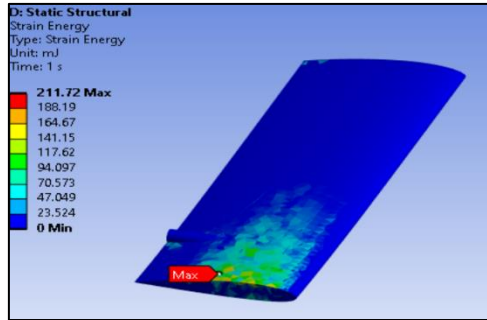


Figure 4.23: Strain Energy of RQ-7 Wing When the Material is Composite, Epoxy/Glass Fiber, UD Prepreg, QI.

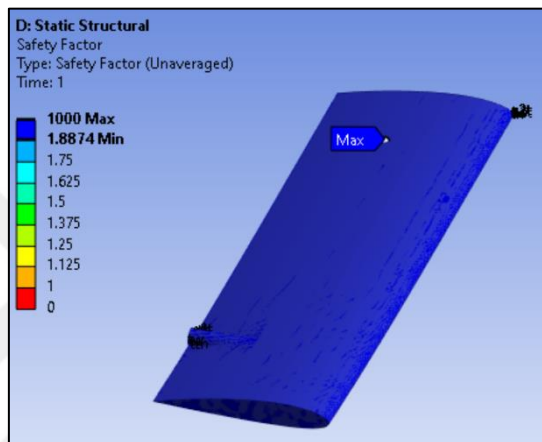


Figure 4.24: Safety Factor of RQ-7 Wing When the Material is Composite, Epoxy/Glass Fiber, UD Prepreg, QI.

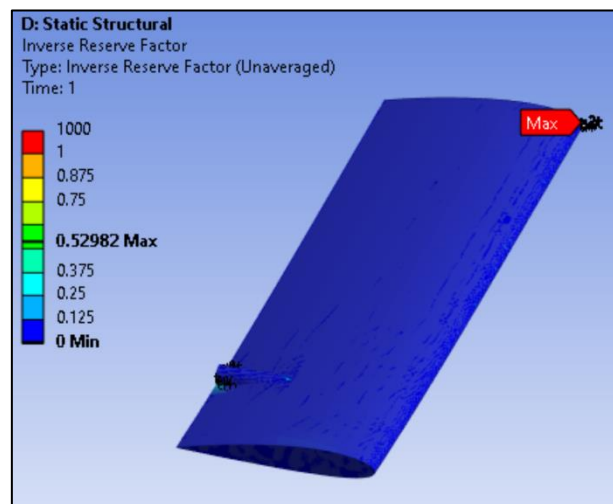


Figure 4.25: Inverse reserve factor of RQ-7 Wing When the Material is Composite, Epoxy/Glass Fibre, UD Prepreg, QI.

Table 4.8: Results of FSI Analysis for Third Case.

Parameter	Value
Maximum Von-mises stress	84.142 (MPa)
Total Deformation	13.646 (MPa)
Elastic strain	0.00269
Strain Energy	211.72 (mJ)
Factor of safety	1.88
Inverse Reserve Factor	0.529

As for the third case, the Maximum Strain criterion was also found to be the most suitable, similarly to the second case, as shown in the tables below.

Table 4.9: Safety Factors Values for Different Criteria's for Third Case.

Criteria	Maximum Stress	Maximum Strain	Tsai-Wu	Tsai-Hill
Safety Factor (SF)	2.033	1.887	1.961	2.011

Table 4.10: Inverse Reserve Factor Values for Different Criteria's for Third Case.

Criteria	Maximum Stress	Maximum Strain	Tsai-Wu	Tsai-Hill
Inverse Reserve Factor (IRF)	0.491	0.529	0.509	0.497

4.4.2 Modal Analysis Results

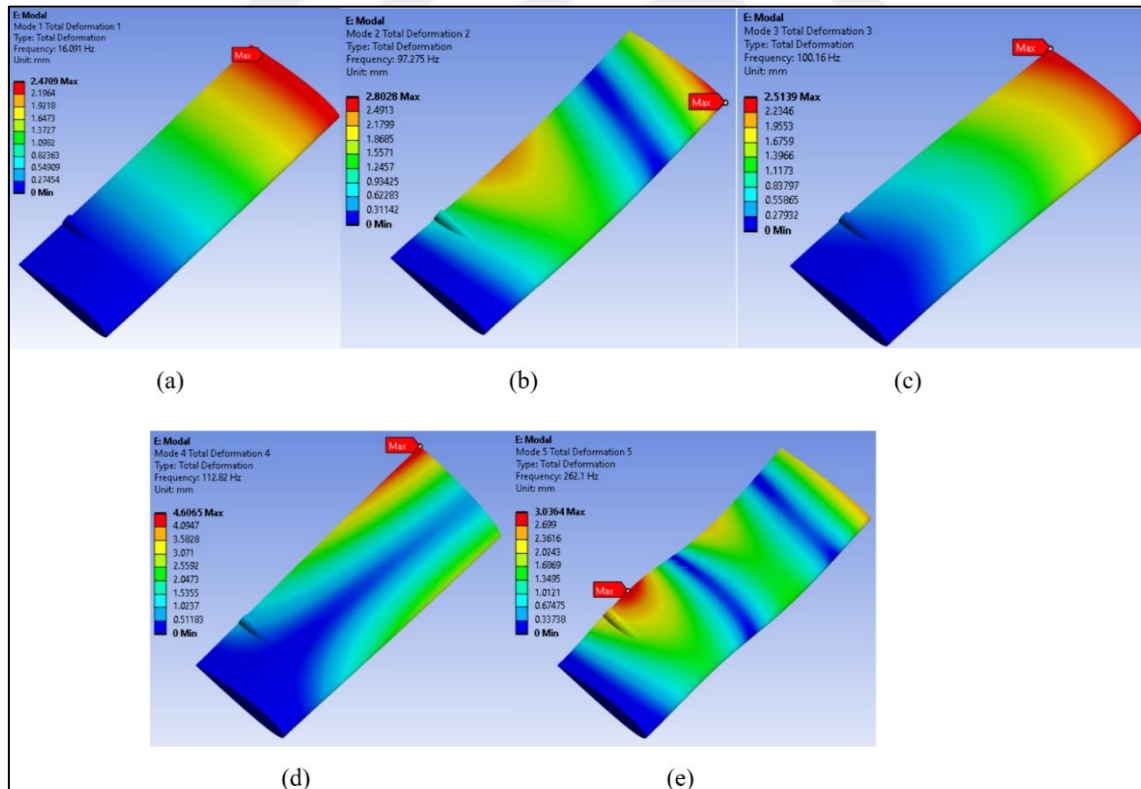


Figure 4.26: Modal Analysis Results of RQ-7 Wing When the Material is Composite, Epoxy/Glass Fiber, UD Prepreg, QI. (a) Mode 1, (b) Mode 2, (c) Mode 3, (d) Mode 4, (e) Mode 5.

Table 4.11: Natural Frequencies of Third Case Study.

Mode	Frequency [Hz]	Total Deformation (mm)
1	16.091	2.47
2	97.275	2.80
3	100.16	2.51
4	112.82	4.60
5	262.1	3.03

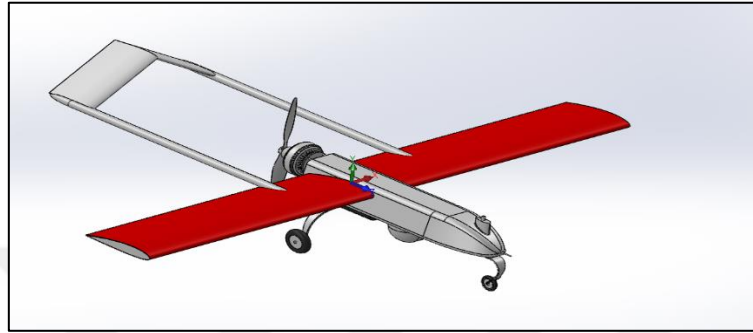


Figure 4.27: AAI Shadow -200 RQ-7 UAV Model After Adding Composite Material.

The results show that both the second and third case studies, using various composite materials, provide good structural performance and address the structural safety requirements. Comparing the second and third cases, the third case using composite material Epoxy/glass fiber, UD prepreg, QI is seen to be superior to the second case that uses Epoxy Carbon UD (230 GPa) Prepreg.

The third case has a higher safety factor (1.88) and a lower inverse reserve factor (0.529) than in the second case, which means better safety margin and higher load-carrying capacity of the applied loads. In addition, the third case shows the lower total deformation (13.646 MPa) in comparison with the second case (15.03 MPa) and indicates the better structural response.

Based on these results, the composite material Epoxy/glass fiber, UD prepreg, QI used in the third case is an advantageous option for the aircraft wing structure. The first-composite material offers superior structural performance, improved safety margins, and better overall economy over the composite material of the second case.

In the context of the modal analysis, the natural frequencies obtained for the second and the third cases were quite close one to another, which means that both composite materials have a similar effect on the vibrational characteristics of the aircraft wing.

5. CONCLUSIONS AND RECOMMENDATIONS

5.1 CONCLUSIONS

The present study has shown the potential of composite materials to improve the structural performance and aerodynamic efficiency of the wings of an aircraft. Using a set of numerical analyses that includes Computational Fluid Dynamics (CFD), Fluid-Structure Interaction (FSI), and modal analysis, the behavior of an AAI Shadow-200 RQ-7 UAV wing in different loading conditions was carefully studied. Therefore, the findings indicate without a doubt that the use of advanced composite materials such as Epoxy Carbon UD Prepreg and Epoxy/glass fiber UD prepreg QI, can greatly improve the wing's ability to withstand the forces exerted by the airflow, thereby, improving its overall performance and reliability.

The use of the latest computational tools and software packages has been the key factor in making this study possible. SOLIDWORKS, in virtue of its strong and user-friendly design capabilities, has allowed to establish a detailed and accurate model of the UAV wing, which served as a sound base for the following numerical simulations. On the other hand, ANSYS has offered a complete set of analysis tools, including CFD, FSI, composite material analysis, and modal analysis modules, which provided a detailed and multi-aspect study of the wing's behavior in different conditions. The perfect incorporation of these advanced computational tools has promoted an inter-disciplinary approach to this research, which has become very informative about the complicated relationships between the wing structure, the surrounding airflow, and the composite materials used.

5.2 RECOMMENDATIONS

- a. Perform testing trials on the prototype or the full-scale model of the AAI Shadow-200 RQ-7 UAV wing with two composite materials examined in this research (Epoxy Carbon UD Prepreg and Epoxy/glass fiber UD prepreg QI) to confirm the numerical results and evaluate the practical possibility of using these materials.
- b. Investigate and evaluate the performance of other composite materials including carbon nanotubes, graphene reinforced polymers and ceramic matrix composites to identify possible materials which could further improve the structural and aerodynamic characteristics of the wing.

- c. Examine the influence of using composite materials in other parts of the AAI Shadow-200 RQ-7 UAV, for instance the fuselage, tail, and control surfaces, on the aircraft's performance and efficiency gains.
- d. Create and verify a multi-objective optimization framework that integrates the numerical analysis tools used in this study (CFD, FSI, composite material analysis, and modal analysis) to simplify the design process and determine the best composite material configurations for particular mission requirements and operational conditions.
- e. Collaborate with industry partners and composite material manufacturers to address the challenges associated with the large-scale production, quality control, and maintenance of composite aircraft components, ensuring the successful transition of the research findings into practical applications.
- f. Investigate the long-term durability, fatigue life, and environmental effects on the composite materials used in the UAV wing to ensure their sustained performance and reliability under various operating conditions. Investigate methods like ultrasonic vibration, surfactant addition, pH control to obtain uniform and durable nanoparticle suspensions.

REFERENCES

- [1] P. G. Fahlstrom and T. J. Gleason, *Introduction to UAV Systems*, 4th ed. West Sussex: Wiley & Sons, Inc., 2012.
- [2] M. Palik and M. Nagy, “Brief history of UAV development,” *Repüléstudományi Közlemények*, vol. 31, no. 1, pp. 155–166, 2019, doi: 10.32560/rk.2019.1.13.
- [3] H. Nawaz, H. M. Ali, and S. Massan, “APPLICATIONS OF UNMANNED AERIAL VEHICLES : A REVIEW,” in *Tecnología. Glosas de innovación aplicadas a la pyme. Edición Especial, Noviembre*, 2019, pp. 85–105. doi: 10.17993/3ctecno.2019.specialissue3.85-105.
- [4] H. Sharma, C. S. Suraj, R. Antony, G. Ramesh, S. Ahmed, and P. Narayan, “Design of a High Altitude Fixed Wing Mini UAV-Aerodynamic Challenges,” 2013.
- [5] F. R. Triputra, B. R. Trilaksono, T. Adiono, R. A. Sasongko, and M. Dahsyat, “Nonlinear Dynamic Modeling of a Fixed-Wing Unmanned Aerial Vehicle: a Case Study of Wulung,” *Journal of Mechatronics, Electrical Power, and Vehicular Technology*, vol. 6, no. 1, pp. 19–30, Jul. 2015, doi: 10.14203/j.mev.2015.v6.19-30.
- [6] M. Bashir, P. Rajendran, C. Sharma, and D. Smrutiranjana, “Investigation of Smart Material Actuators & Aerodynamic optimization of Morphing Wing,” *Mater Today Proc*, vol. 5, no. 10, pp. 21069–21075, 2018, doi: 10.1016/j.matpr.2018.06.501.
- [7] J. Yu, “Design and Optimization of Wing Structure for a Fixed-Wing Unmanned Aerial Vehicle (UAV),” *Modern Mechanical Engineering*, vol. 08, no. 04, pp. 249–263, 2018, doi: 10.4236/mme.2018.84017.
- [8] H. Yu, W. Yang, H. Duan, and A. S. Malik, “Flexibility distribution tuning by wing frame inner structure morphing for fixed-wing unmanned aerial vehicle,” in *AIAA Aviation 2019 Forum*, American Institute of Aeronautics and Astronautics Inc, AIAA, 2019, pp. 1–12. doi: 10.2514/6.2019-3348.

- [9] A. Altememe, O. J. Myers, and A. Hall, "Computational Fluid Dynamic Analysis of Flapping Wing of Micro Aerial Vehicle at Very Low Reynolds Numbers Turbulent Flow," *International Journal of Aeronautics and Aerospace Engineering*, vol. 1, no. 2, pp. 68–75, Aug. 2019, doi: 10.18689/ijae-1000110.
- [10] A. Altememe, O. J. Myers, and A. Hall, "Preliminary Design and Computational Fluid Dynamic analysis of Flapping Wing of Micro Aerial Vehicle for Low Reynolds Numbers Regime," *International Journal of Aeronautics and Aerospace Engineering*, vol. 1, no. 2, pp. 36–45, May 2019, doi: 10.18689/ijae-1000106.
- [11] T. K. Priyambodo and A. Majid, "Modeling and Simulation of The UX-6 Fixed-Wing Unmanned Aerial Vehicle," *Journal of Control, Automation and Electrical Systems*, vol. 32, no. 5, pp. 1344–1355, Oct. 2021, doi: 10.1007/s40313-021-00754-5.
- [12] S. Syam Narayanan, R. A. Ahmed, M. E. Varshini, V. B. Rao, and S. Kyathiswar, "One-way fluid-material interaction study on a plunging UAV wing," in *Materials Today: Proceedings*, Elsevier Ltd, 2021, pp. 316–320. doi: 10.1016/j.matpr.2021.07.408.
- [13] N. Muhammad, Z. Fang, and Y. Cao, "Fatigue life estimation of fixed-wing unmanned aerial vehicle engine by grey forecasting," *Measurement and Control (United Kingdom)*, vol. 54, no. 5–6, pp. 799–810, May 2021, doi: 10.1177/0020294020915215.
- [14] H. Zhu *et al.*, "Fluid–structure interaction-based aerodynamic modeling for flight dynamics simulation of parafoil system," *Nonlinear Dyn*, vol. 104, no. 4, pp. 3445–3466, Jun. 2021, doi: 10.1007/s11071-021-06486-0.
- [15] J. O. Imumbhon, M. Landazuri, and Y. Cao, "Structural and CFD analyses of a reciprocating-airfoil (RA) driven UAV wing under maximum lift and inertia forces," *Drone Systems and Applications*, vol. 10, no. 1, pp. 287–308, Jan. 2022, doi: 10.1139/dsa-2021-0043.

- [16] A. Irsalan, R. C. K. Leung, G. C. Y. Lam, and M. R. Naseer, “Fluid-structure interactions and aeroacoustic coupling of airfoil with flexible membrane(s),” in *Internoise 2022 - 51st International Congress and Exposition on Noise Control Engineering*, The Institute of Noise Control Engineering of the USA, Inc., 2023, pp. 1–13. doi: 10.3397/in_2022_0594.
- [17] A. N *et al.*, “Design and analysis of a tail sitter (VTOL) UAV composite wing,” *Mater Today Proc*, vol. 56, pp. 1604–1613, 2022, doi: 10.1016/j.matpr.2022.03.231.
- [18] E. I. Basri, A. A. Basri, S. Balakrishnan, M. T. H. H. Sultan, and K. A. Ahmad, “Performance analysis of composite laminates wing skin with the aid of fluid structure interaction of aerodynamic loading-structural analysis,” *Mechanics Based Design of Structures and Machines*, vol. 52, no. 2, pp. 922–942, 2022, doi: 10.1080/15397734.2022.2126983.
- [19] H. Yang, S. Jiang, Y. Wang, and H. Xiao, “Design, kinematic and fluid-structure interaction analysis of a morphing wing,” *Aerosp Sci Technol*, vol. 143, Dec. 2023, doi: 10.1016/j.ast.2023.108721.
- [20] H. Li, Z. Wang, D. Li, Z. Tu, S. Zhao, and Z. Kan, “Fluid-structure analysis of flapping-wing rotorcraft considering stiffness influence,” *Aerosp Sci Technol*, vol. 143, pp. 1–14, Dec. 2023, doi: 10.1016/j.ast.2023.108728.
- [21] M. El Adawy *et al.*, “Design and fabrication of a fixed-wing Unmanned Aerial Vehicle (UAV),” *Ain Shams Engineering Journal*, vol. 14, no. 9, pp. 1–17, Sep. 2023, doi: 10.1016/j.asej.2022.102094.
- [22] A. Porta Ko, S. Smidt, R. Schmehl, and M. Mandru, “Optimisation of a Multi-Element Airfoil for a Fixed-Wing Airborne Wind Energy System,” *Energies (Basel)*, vol. 16, no. 8, pp. 1–18, Apr. 2023, doi: 10.3390/en16083521.
- [23] N. Pynaert, T. Haas, J. Wauters, G. Crevecoeur, and J. Degroote, “Wing Deformation of an Airborne Wind Energy System in Crosswind Flight Using High-Fidelity Fluid–Structure Interaction,” *Energies (Basel)*, vol. 16, no. 2, pp. 1–16, Jan. 2023, doi: 10.3390/en16020602.

- [24] Rashmikant, M. Onishi, K. Sugikawa, and D. Ishihara, “Computational evaluation of flight performance of flapping-wing nano air vehicles using hierarchical coupling of nonlinear dynamic and fluid-structure interaction analyses,” *Engineering Applications of Computational Fluid Mechanics*, vol. 17, no. 1, pp. 1–20, 2023, doi: 10.1080/19942060.2023.2271053.
- [25] H. Zhu *et al.*, “Fluid-structure interaction simulation for performance prediction and design optimization of parafoils,” *Engineering Applications of Computational Fluid Mechanics*, vol. 17, no. 1, 2023, doi: 10.1080/19942060.2023.2194359.
- [26] P. Caccavale, B. Mele, M. Brandizzi, and G. Ruocco, “Fully Coupled Fluid–Structure Interaction with Heat Transfer Effects in an Adaptive NACA Airfoil,” *Fluids*, vol. 8, no. 2, pp. 1–12, Feb. 2023, doi: 10.3390/fluids8020039.
- [27] D. Ishihara and M. Onishi, “Computational fluid–structure interaction framework for passive feathering and cambering in flapping insect wings,” *Int J Numer Methods Fluids*, vol. 96, no. 5, pp. 435–481, Apr. 2023, doi: 10.1002/flid.5251.
- [28] X. Bai, “Study and analysis of lift to drag ratio performance of supercritical wing based on computational fluid dynamics method,” in *Journal of Physics: Conference Series*, Institute of Physics, 2023, pp. 1–14. doi: 10.1088/1742-6596/2634/1/012018.
- [29] S. Tao, “Numerical Simulation of the Influence of Ski-jump Deck on the Take-Off Zone Flow Field Based on CFD,” in *Journal of Physics: Conference Series*, Institute of Physics, 2023. doi: 10.1088/1742-6596/2599/1/012049.
- [30] M. Luo, Z. Wu, and C. Yang, “Strongly coupled fluid–structure interaction analysis of aquatic flapping wings based on flexible multibody dynamics and the modified unsteady vortex lattice method,” *Ocean Engineering*, vol. 281, pp. 1–14, Aug. 2023, doi: 10.1016/j.oceaneng.2023.114921.
- [31] Y. Wang, P. Lei, B. Lv, Y. Li, and H. Guo, “Study on Fluid–Structure Interaction of a Camber Morphing Wing,” *Vibration*, vol. 6, no. 4, pp. 1060–1074, Dec. 2023, doi: 10.3390/vibration6040062.

- [32] S. Vijayalakshmi *et al.*, “Multi-perspective structural integrity-based computational investigations on airframe of Gyrodyne-configured multi-rotor UAV through coupled CFD and FEA approaches for various lightweight sandwich composites and alloys,” *Reviews on Advanced Materials Science*, vol. 62, no. 1, pp. 1–49, Jan. 2023, doi: 10.1515/rams-2023-0147.
- [33] I. Kostić, A. Simonović, O. Kostić, D. Ivković, and D. Tanović, “Lateral-Directional Aerodynamic Optimization of a Tandem Wing UAV Using CFD Analyses,” *Aerospace*, vol. 11, no. 3, pp. 1–20, Mar. 2024, doi: 10.3390/aerospace11030223.
- [34] M. R. Rajanna *et al.*, “Fluid–structure interaction modeling with nonmatching interface discretizations for compressible flow problems: simulating aircraft tail buffeting,” *Comput Mech*, pp. 1–11, 2024, doi: 10.1007/s00466-023-02436-2.
- [35] A. Psarros *et al.*, “Detail and structural design of a fixed-wing BWB UAV,” *J Phys Conf Ser*, vol. 2716, no. 1, pp. 1–9, Mar. 2024, doi: 10.1088/1742-6596/2716/1/012069.
- [36] K. Marangi and S. M. Salim, “Predicting the Structural Performance of the Wings of an Unmanned Aircraft Vehicle Using Fluid-structure Interaction,” in *Proceedings of the World Congress on Engineering 2019*, 2019, pp. 1–6.
- [37] H. YU, “NUMERICAL SIMULATIONS OF STRUCTURAL AND FLUID DYNAMICS FOR AERODYNAMIC PERFORMANCE IMPROVEMENT,” UNIVERSITY OF TEXAS AT DALLAS, 2021.
- [38] F. CELEN, “INVESTIGATION OF EFFECT OF MASS DISTRIBUTION ON WING FLUTTER BY FLUID-STRUCTURE INTERACTION ANALYSIS,” MIDDLE EAST TECHNICAL UNIVERSITY, 2022.
- [39] S. Rahman and A. Ranganathan, “Conceptual design and construction of a UAV wing structure,” EXAMENSARBETE INOM TEKNIK, 2020.

- [40] B. D. O. Taye Stephen Mogaji Adegoke Ezekiel Fadiji, “Design and CFD Analysis of a Fixed-Wing Unmanned Aerial Vehicle Wing Unmanned Aerial Vehicle for Surveillance Purpose,” *International Journal of Engineering and Emerging Scientific Discovery*, vol. 7, no. 3, pp. 23–36, 2022.
- [41] R. Poletti, M. Barucca, L. Koloszar, M. A. Mendez, and J. Degroote, “DEVELOPMENT OF AN FSI ENVIRONMENT FOR THE AERODYNAMIC PERFORMANCE ASSESSMENT OF FLAPPING WINGS,” in *International Conference on Computational Methods for Coupled Problems in Science and Engineering*, 2023, pp. 1–12.
- [42] V. Raja *et al.*, “Design, Computational Aerodynamic, Aerostructural, and Control Stability Investigations of VTOL-Configured Hybrid Blended Wing Body-Based Unmanned Aerial Vehicle for Intruder Inspections,” *International Journal of Aerospace Engineering*, vol. 2023, pp. 1–31, 2023, doi: 10.1155/2023/9699908.
- [43] S. Vlachos, C. Pliakos, C. Bliamis, and K. Yakinthos, “CFD aided investigation of a three-blade propeller in multirotor UAV applications,” *J Phys Conf Ser*, vol. 2716, no. 2024, pp. 1–8, 2024, doi: 10.1088/1742-6596/2716/1/012064.
- [44] P. Longobardi and J. Skaloud, “Aerodynamic modeling of a delta-wing UAV for model-based navigation,” *CEAS Aeronaut J*, pp. 1–19, 2024, doi: 10.1007/s13272-024-00727-9.
- [45] J. D. Anderson and C. P. Cadou, *Fundamentals of Aerodynamics*, 7th ed., vol. 5, no. March. New York: McGraw-Hill, 2024. [Online]. Available: <https://www.crcpress.com/Fundamentals-of-Picoscience/Sattler/p/book/9781466505094#googlePreviewContainer>
- [46] F. M. White and H. Xue, *FLUID MECHANICS*, 9th ed. New York: McGraw-Hill, 2021.

- [47] H. Anam, L. Haris, A. Budiarto, and A. Budiyo, “Design of Diver Propulsion Vehicle Ganendra RI-1 Using SolidWorks Flow Simulation,” *Marine and Underwater Science and Technology*, no. December, pp. 55–60, 2015.
- [48] A. Kabir, M. S. Chowdhury, M. J. Islam, and M. Islam, “Numerical Assessment of the Backward Facing Step for NACA 0015 Airfoil using Computational Fluid Dynamics,” in *1st International Conference on Advances in Science, Engineering and Robotics Technology 2019, ICASERT 2019*, 2019. doi: 10.1109/ICASERT.2019.8934501.
- [49] F. J.H., P. M., and R. L. Street, *Computational Methods for Fluid Dynamics*, 4th ed. Gewerbestrasse: Springer Nature Switzerland AG, 2020. doi: 10.1063/1.2815085.
- [50] R. Saini and C. Buchser, “An introduction to computational fluid dynamics for manufacturing - CRB,” Crb Group. [Online]. Available: <https://www.crbgroup.com/insights/consulting/introduction-computational-fluid-dynamics>
- [51] J. BLAZEK, *Computational fluid dynamics principles and applications*, 3rd ed. Oxford OX5: Elsevier, 2015.
- [52] M. Ezkurra *et al.*, “Analysis of One-Way and Two-Way FSI Approaches to Characterise the Flow Regime and the Mechanical Behaviour during Closing Manoeuvring Operation of a Butterfly Valve,” *International Journal of Mechanical and Materials Engineering*, vol. 12, no. 4, pp. 409–415, 2018, [Online]. Available: <https://www.researchgate.net/publication/325170283>
- [53] N. Schmitz, M. Hellenkamp, H. Pfeifer, E. Cresci, J. Wüning, and M. Schönfelder, “Radiant Tube life improvement for vertical galvanizing lines,” in *Iron and Steel Technology*, 2016, pp. 67–73.
- [54] D. L. Logan, *A First Course in the Finite Element Method*, 6th ed. Boston: Cengage, 2023.

- [55] S. Moaveni, *Finite Element Analysis Theory and Applications with ANSYS*, 4th ed. Essex: Pearson Education Limited, 2014. doi: 10.1016/0010-4485(84)90036-8.
- [56] M. A. Rao, M. R. Khanna, K. J. Somaiya, and M. Gangopadhyay, "Applications of Finite Elements Method (FEM) - An Overview," *International Conference on Mathematical Sciences*, vol. 28, no. 31, pp. 1–8, 2012, doi: 10.13140/RG.2.2.36294.42565.
- [57] E. M. Alawadhi, *Finite Element Simulations Using ANSYS*, 2nd ed. Broken: CRC Press Taylor & Francis, 2016. doi: 10.1201/b18949.
- [58] R. F. Gibson, *PRINCIPLES OF MECHANICS MATERIAL COMPOSITE*, 4th ed. Ohio: Taylor & Francis Group, LLC, 2016.
- [59] G. Sumithra, R. N. Reddy, G. Dheeraj Kumar, S. Ojha, G. Jayachandra, and G. Raghavendra, "Review on composite classification, manufacturing, and applications," *Mater Today Proc*, no. xxxx, 2023, doi: 10.1016/j.matpr.2023.04.637.
- [60] M. Bhong *et al.*, "Review of composite materials and applications," *Mater Today Proc*, no. June, 2023, doi: 10.1016/j.matpr.2023.10.026.
- [61] Budynas Richard G. and Nisbett J. Keith, *Shigley's Mechanical Engineering Design*, 11th ed. New York: Mc Hall Education, 2020. [Online]. Available: <http://www.elsevier.com/locate/scp>
- [62] M. I. Ali and J. Anjaneyulu, "Effect of fiber-matrix volume fraction and fiber orientation on the design of composite suspension system," in *IOP Conference Series: Materials Science and Engineering*, 2018, p. 012104. doi: 10.1088/1757-899X/455/1/012104.
- [63] N. F. Saari *et al.*, "Estimating natural frequency of pipe with various geometries: Improvement of frequency factors," *Heliyon*, vol. 10, no. 4, p. e26148, 2024, doi: 10.1016/j.heliyon.2024.e26148.

- [64] M. M. S. Reza, S. A. Mahmood, and A. Iqbal, "Performance Analysis and Comparison of High Lift Airfoil for Low-Speed Unmanned Aerial Vehicle," in *International Conference on Mechanical, Industrial and Energy Engineering 2016*, 2016, pp. 1–8. [Online]. Available: <https://doi.org/10.5281/zenodo.1468120>
- [65] G. E. Corporation, "GEC Delivers Weight & Balance Kits For The UAV RQ-7 Shadow Aircraft," weighing review. [Online]. Available: <https://www.weighingreview.com/article/gec-delivers-weight-balance-kits-for-the-uav-rq-7-shadow-aircraft>
- [66] Z. Siddiqi and J. W. Lee, "A computational fluid dynamics investigation of subsonic wing designs for unmanned aerial vehicle application," *Proc Inst Mech Eng G J Aerosp Eng*, vol. June 2019, no. June 2019, pp. 1–10, 2019, doi: 10.1177/0954410019852553.
- [67] A. Khaliq, M. A. Kamran, and M. Y. Jeong, "Nanoimprint Mold Consisting of an Adhesive Lap Joint between a Nanopatterned Metal Sleeve and a Carbon Composite Roll Amin," *Nanomaterials*, vol. 13, no. 10, pp. 1–14, 2023, doi: 10.3390/nano13101685.
- [68] C. 2018 EDUPACK, "Epoxy/S-glass fiber, UD prepreg, QI lay-up," 2019. [Online]. Available: https://www.researchgate.net/profile/Janos-Plocher/post/Does_increasing_glass_fiber_weight_percentage_volume_fraction_increase_Modulus_in_GFRP_composites/attachment/5c1cdb4dcfe4a764550a8b6d/AS%3A706252061564928%401545395021690/download/Material+Data~Epoxy.